This is to certify that the
thesis entitled

ANALYSIS AND DESIGN OF RESONANT FREQUENCY CONTROL SYSTEMS WITH APPLICATIONS

presented by

Daniel Smith

has been accepted towards fulfillment
of the requirements for the

M.S. degree in Mechanical Engineering

C. Gahuch
Major Professor's Signature

5/8/07
Date

ANALYSIS AND DESIGN OF RESONANT FREQUENCY CONTROL SYSTEMS WITH APPLICATIONS

By

Daniel Smith

A THESIS

Submitted to
Michigan State University
in partial fulfillment of the requirements
for the degree of

MASTER OF SCIENCE

Mechanical Engineering

2007

ABSTRACT

ANALYSIS AND DESIGN OF RESONANT FREQUENCY CONTROL SYSTEMS WITH APPLICATIONS

By

Daniel Smith

Resonant systems arise in many areas throughout science and engineering. Some examples of systems which must be excited at resonance for optimal performance include ultrasonic motors, inductive heating loads, cavity resonators, and cyclotrons. Due to disturbances such as environmental conditions, load variation and degradation, the resonant frequency of these systems can shift, resulting in loss of performance. This necessitates employment of a resonant frequency control system that maintains lock between the excitation frequency and the resonant frequency.

In this thesis, three resonant frequency control methods are investigated. The first uses nonlinear feedback with a phase lead compensator to start and sustain oscillation at the resonant frequency of the system. The second method varies the excitation frequency to track the resonant frequency of the system by seeking the frequency corresponding to a local maximum of the magnitude response. The third method varies a parameter in the resonant system to tune the resonant frequency to the excitation frequency by seeking the parameter value corresponding to a local maximum of the magnitude response. Non-linear models of these control systems are developed and linearized to obtain tractable models for analysis and design. In addition, design guidelines are provided and results are illustrated through two applications: a novel RF plasma ignition system, and a dynamic vibration absorber. Simulation results are presented for the dynamic vibration absorber and the developed RF plasma ignition system to illustrate the effectiveness of the proposed control methods. Also, experimental results for the proposed ignition system are presented to further demonstrate the features of the proposed methods and the viability of the ignition system.

This work is dedicated to my family, who has made it possible for me to become the person I am today.

ACKNOWLEDGMENTS

I would like to acknowledge my advisor, Dr. Cevat Gökçek, for his generous investment of expertise and time, and for his dedication to my development. His mentoring has contributed immensely to my personal and professional growth and will have lifelong impact. Also, I would like to thank Dr. Harold Schock and his staff for providing resources which made engine testing of the RF plasma ignition system possible. In addition, I would like to thank my family and friends for their support and understanding through this endeavor.

TABLE OF CONTENTS

LIST OF FIGURES

CHAPTER 1

Introduction

Resonant systems are found commonly throughout the disciplines of science and engineering. In many cases resonance is destructive, and therefore should be avoided. In some systems, however, resonance is useful, if not critical for proper operation of a system. Maintaining resonance may be difficult since operating conditions, wear, aging, manufacturing defects and other disturbances often cause the resonant frequency or excitation frequency of such systems to vary. *Resonant frequency control* methods are therefore proposed in this work which compensate for these variations to ensure oscillation at the resonant frequency of the resonator. Resonant frequency control is based on two approaches: tracking the resonant frequency of a system by varying the excitation frequency, referred to as *resonance tracking control*, and by varying the resonant frequency of the system to track the excitation frequency, referred to as *resonance tuning control*. The aim of this thesis is to develop systematic modeling, analysis and design methods for resonant frequency control systems and to apply them to two applications to demonstrate that the methods are effective and useful. Three resonant frequency control methods are presented; two are based on resonance seeking control methods, and one on resonance tuning control methods. In addition, two applications for these methods, an RF plasma ignition system, and a dynamic vibration absorber are presented.

This section will discuss the motivation and applications for the research on reso-

nance seeking control, as well as briefly discuss the methods that have been developed to solve this problem.

1.1 Motivation

Resonant loads, such as ultrasonic motors, piezoelectric transducers, induction heating loads, resonant inverter loads, microelectromechanical gyroscopes, cyclotrons, cavity resonators, microwave heating loads, plasma processing loads and bandpass wireless communication loads, arise in several areas of science and engineering [1]-[20]. Such loads must be driven at their resonant frequencies for optimal performance [1]-[20]. However, even if these loads are driven initially at their resonant frequencies, disturbances, such as temperature change, load variation, manufacturing variability, aging, fatigue damage, microphonics or electromagnetic detuning, can cause their resonant or excitation frequencies to drift with time and significantly impair their performance. This necessitates employment of resonant frequency control systems that excites such systems at their resonant frequencies or tune the resonant frequency of the system to the excitation frequency in the face of such inherent disturbances.

The lock between the excitation frequency and resonant frequency of a resonant system can be achieved by tracking the resonant frequency and varying the excitation frequency accordingly to match the resonant frequency. Alternatively, the resonant frequency of the resonant system can be tuned to match the excitation frequency. It should be pointed out that in some applications (ultrasonic motors, piezoelectric transducers, induction heating loads, resonant inverter loads, microwave heating loads and plasma processing loads) the former approach is more feasible while in some other applications (microelectromechanical gyroscopes, cavity resonators, cyclotrons and bandpass wireless communication loads) the latter approach is more feasible.

The resonance frequency control problem has received significant attention recently in the contexts of the specific applications listed above. When the model of

the resonator is a lightly damped second order system, the phase of its impedance or admittance function is locally odd about the resonant frequency and its value is 0, $\pi/2$, or $-\pi/2$ rad at the resonant frequency. Thus, for such resonators, the phase characteristic of its transfer function measured by a phase detector can be used for resonance seeking control purposes. Recent resonant frequency control methods with general formulations for second order systems which take advantage of this characteristic are as follows. In [21], analysis and design methods are developed for a resonance tracking control method for resonating an RLC circuit using phase-locked loop. In [22] resonance tracking is achieved by using proportional feedback around the second order system and adaptively controlling the feedback gain using the error between the excitation and resonant frequencies obtained by a phase detector. In [23] a resonance tuning control method is developed for second order systems, in which a system parameter is adaptively tuned to change the resonant frequency of the resonator, again using phase detection. In many practical cases, however, the order of the system is often inherently higher than two. In these situations, the phase detector based resonance seeking control method is usually inadequate. Further methods suitable for a broader range of resonant systems are desirable. Therefore, the goal of this thesis is to introduce and investigate control methods that seek the unknown resonant frequency of a system and drive it at its resonant frequency, and to apply such tools to two applications, an RF plasma ignition system and a dynamic vibration absorber.

1.1.1 RF Plasma Ignition System

Modern spark ignited internal combustion engines are required to minimize exhaust emissions while maximizing fuel efficiency. These requirements call for precise control of the ignition timing to run the engine at the knock threshold and the ignition energy to improve the combustion efficiency. The effects of ignition energy and timing on combustion quality have been widely studied. Increasing ignition energy and

precisely controlling its timing have been shown to reduce combustion delay, rise time, unwanted emissions and cycle-to-cycle variability while increasing lean limits, knock limits and efficiency [24]–[26]. Thus the ignition system plays a crucial role in the optimal operation of modern engines.

Ignition systems have been incrementally refined for many years. Their basic nature, however, has remained essentially unchanged and their energy transfer efficiency is still extremely low (less than 1%) [24]. As a result, the spark generated by conventional ignition systems is usually weak, stationary and confined between the two electrodes of the spark plug. The weak and stationary spark causes slow or incomplete burn of the air-fuel mixture resulting in low fuel economy, high emissions, and reduced power [27]–[30]. With these conventional ignition systems, the achievable lean limit and exhaust gas recirculation tolerances are also modest [27]–[30]. Further, the performance of conventional ignition systems is known to deteriorate especially during cold start or with fouled spark plugs [24].

Competition among automotive manufacturers as well as government regulations for better performance necessitate development of new ignition systems that may overcome the shortcomings of conventional ignition systems. Recent efforts toward this goal have focused on modifications to conventional ignition systems [31]–[34]. All of these efforts, however, are still hindered by poor spark plug longevity and inherently low efficiency due to high secondary coil resistance. Other non-conventional efforts include using a high frequency transformer to achieve high voltage for ignition [35], using an RF resonator for this purpose [36], and utilizing a pulsed high power laser beam focused through a window into the combustion chamber for ignition [37]. Systems utilizing a high frequency transformer still have a relatively low operating frequency resulting in performance similar to that of a conventional ignition systems. RF resonators lack robustness since slight component variations easily detune the resonator, resulting in inadequate voltage. Laser induced ignition is not feasible in

automotive applications due to its high power and optical accessibility to cylinder requirements. As a result, none of these ignition systems have found widespread applications in automotive industry.

An RF plasma torch is a viable and promising ignition system for achieving increased ignition energy and precisely controlled ignition timing [38], [39]. This type of ignition systems uses a high quality factor RF resonator excited by an RF generator to start and sustain an RF plasma torch for a prescribed duration inside the combustion chamber. Plasmas can be classified as DC, AC and RF plasmas according to their excitation frequency f. For a spacing between the electrodes of a few millimeters, the classification is roughly as follows. When $f < 1$ kHz, the generated plasma is turned off between the excitation cycles: and this type of plasma is called a DC plasma. When 10 kHz $< f <$ 1 MHz, the generated plasma is on continuously but the ions cross the sheath in less than one excitation cycle and follow the instantaneous sheath potential. This type of plasma is called an AC plasma. When $f >$ 10 MHz, the plasma is on continuously and it takes many excitation cycles to cross the sheath region. This type of plasma is called a RF plasma. Concerning ignition systems, the plasma generated by a conventional ignition system is a DC plasma.

The DC plasma requires a large sheath voltage. Its efficiency is low since a considerable amount of energy is dissipated in non-ionizing collisions. For the RF plasma, the sheath size changes with each RF cycle that moves the charged particles back and forth through the plasma. This displacement current generates heat dissipation that is proportional to the square of the frequency. Hence, the efficiency of the RF plasma is very high. The efficiency of an AC plasma lies between that of a DC plasma and a RF plasma. It is generally easier to control the plasma density and the peak ion bombardment energy with RF excitation.

In this work an RF plasma torch is employed to ignite and initiate controlled combustion. It is believed that RF plasma ignition has several advantages over con-

ventional technologies. The proposed RF ignition system is expected to: (1) accelerate the initial flame development by lowering the effective ignition temperature and time, thus decreasing heat losses to the chamber walls, resulting in higher overall thermal efficiency as well as a faster and more powerful burn; (2) provide a better match with the ionization and dissociation energies of the molecules present in the combustion chamber, resulting in lowered radiation and conduction heat losses; (3) have beneficial effects on the fuel decomposition rates prior to combustion; (4) reduce the troublesome spark advance requirement due to the precise control of ignition timing and energy; (5) extend the lean limit and enhance the EGR tolerance by precisely adjusting the plasma power and its duration according to engine operating conditions; (6) yield reduced electrode wear and spark plug fouling as a result of RF excitation; and (7) cause low electromagnetic interference.

RF plasma is generated by the ignition system without the need for a ground electrode, and develops as a large, spider shaped corona discharges emanating from the regions of highest electromagnetic field strength. Despite all of its potential benefits, this ignition system requires its RF resonator to be excited precisely at its resonant frequency to generate the plasma torch. Thus, it is extremely sensitive to environmental changes and manufacturing tolerances. Hence, for proper practical operation, it requires a control system to track the resonant frequency of the resonator and drive it at that frequency despite environmental changes and manufacturing tolerances.

To demonstrate the event that such a system can generate, Figure 1.1 shows a corona discharge from the system. This discharge contains a number of plasma streamers that are caused by 'avalanches' of ions. When a high electromagnetic field periodically draws in or pushes away ions, they collide with other molecules generating more ions that in turn are pushed and pulled away, creating an avalanche effect. Corona discharges are therefore capable of dispensing energy into a much larger

volume than arc-based ignition systems, where the current flow naturally concentrates into the path generated at breakdown. Failure of the system to properly track the resonant frequency will either severely degrade such a discharge, or will prevent the discharge completely.

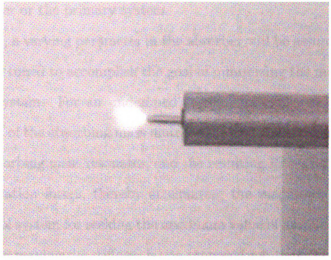

Figure 1.1. Corona discharge from bench testing.

Such a discharge is inherently more efficient, and has potential to significantly improve combustion with a resulting increase and power and reduction in emissions. Due to the simplicity and effectiveness of the system proposed, it offers excellent potential for automotive ignition systems, as well as many other applications. Thus, developing resonance frequency control methods suitable for such a system will make the concept viable, and will potentially provide a significant contribution toward automotive engine technology.

1.1.2 Dynamic Vibration Absorber

The second example presented is a classical dynamic vibration absorber problem consisting of a sinusoidally excited mass-spring-damper (MSD) with a tuned absorber attached. In this configuration, a properly tuned absorber can effectively attenuate the sinusoidal force exerted on the primary system. However, it is assumed that the

excitation frequency or system parameters are not precisely known. With known values, properly tuning an absorber is a relatively easy. However, if the variables are not precisely known, it is necessary to implement a control system that will adjust the absorber parameters to accommodate for deviations in the parameter values of either the absorber or the primary system.

For this thesis, a varying parameter in the absorber will be assumed [40]-[44]. This parameter will be tuned to accomplish the goal of minimizing the magnitude response of the primary system. For an undamped system, minimization occurs when the natural frequency of the absorbing mass matches the excitation frequency [45]. At this condition the absorbing mass resonates, and the resulting forces on the original mass counter the excitation forces, thereby attenuating the magnitude response. Thus, designing a control system for seeking the maximum value of amplitude of the isolated absorbing MSD by varying the stiffness is one proposed solution. Therefore the design problem is not varying the frequency of excitation, but rather adapting the parameters of the absorber to attenuate vibration in the primary system.

1.2 Problem Formulation

Considering the motivation and applications discussed above, the following resonant frequency control problem is formulated: Given a resonator, develop a model which includes the resonator and an appropriate resonant frequency control system. Then determine the performance of the feedback system (stability, robustness, disturbance rejection, reference tracking, rise time, settling time, maximum overshoot, etc.). Finally, design the parameters of the overall system so that the system achieves certain desired performance objectives.

This problem is motivated by two classifications of resonant systems: second order systems and higher order systems. For each type of resonator, this thesis will present an appropriate resonant frequency control system. The resonant frequency control

systems will be demonstrated with simulation results, and with experimental results from the RF plasma ignition system.

1.3 Resonant Frequency Control Systems

As mentioned above, two approaches to solving the resonant frequency control problem are considered in this work. First, resonance tracking control is considered, where the resonant system is excited at its resonance frequency by varying the excitation frequency. Second, resonance tuning control is considered, where a structural parameter in the system is varied to tune the resonant frequency of the resonator to the excitation frequency. The first method that will be presented is *self-oscillating resonance tracking systems*, and is a form of resonance tracking control. This method primarily well suited to second order resonators. The second method that will be proposed is an adaptive control method which tracks the resonant frequency of the resonant system by controlling the frequency of excitation. This method is thus a form of resonance tracking control, and will be referred to as *resonance seeking control.* The third method is also and adaptive control method, but varies a parameter of the resonant system to tune the resonant frequency to the excitation frequency. This method is therefore will be referred to as *resonance tuning control.* These last two methods are suitable for higher order resonators, but may also be used for resonant frequency control of second order systems.

1.3.1 Self-Oscillating Resonance Tracking Control

Self-oscillating resonance tracking control is a method by which resonant systems self-start and sustain oscillation. Feedback is designed with two elements: a compensator, which is designed to compensate for phase changes in the loop, and a nonlinearity, which is designed to provide self-starting ability and an amplitude limitation mechanism. The describing function method [46] will be used to determine the conditions

necessary for resonance, and design guidelines will be given for designing the compensator and nonlinearity. This resonant frequency control method is well-suited for second order systems, and the main analysis and design methods in this work include a time delay as found in the RF plasma ignition system. Design of compensators suitable for higher order systems will also be briefly discussed.

1.3.2 Resonance Seeking Control

Resonance seeking control is an adaptive method based on that found in [47] that seeks the frequency corresponding to a local maximum in the magnitude response of a system. The system is excited with a variable frequency oscillator. The frequency of the sinusoid is controlled through feedback by estimating the derivative of the magnitude response of the resonant system with respect to the excitation frequency. From this derivative, the frequency corresponding to the local maximum value of the magnitude response of the system can easily be sought. The derivative is estimated by perturbing the excitation frequency of the resonant system with a low amplitude, low frequency sinusoid, then synchronously demodulating the absolute value of the output of the system. After being filtered, the signal is fed back to complete the control loop. The low pass filter used for synchronous demodulation plays the role of the controller in the system, thus design methods focus primarily on this element.

1.3.3 Resonance Tuning Control

Resonance tuning control is also an adaptive method that seeks a parameter value of the resonant system corresponding to a local maximum in the magnitude response. The resonant system is excited with a fixed amplitude, fixed frequency sinusoidal signal. The variable system parameter is controlled through feedback by estimating the derivative of the magnitude response of the resonant system with respect to the adjustable parameter value from which the maximum value can easily be sought. The

derivative is estimated by perturbing the adjustable parameter value of the system with a low amplitude, low frequency sinusoid, then synchronously demodulating the absolute value of the output of the system. After being filtered, the signal is fed back to complete the control loop. Again, the low pass filter used for synchronous demodulation plays the role of the controller in the system, thus design methods focus primarily on this element.

1.4 Thesis Overview

1.4.1 Thesis Organization

This thesis is organized as follows: Chapter 2 provides the models of the resonant frequency control systems as well as models for the motivating application. Chapter 3 presents analysis of the resonant frequency control methods. Chapter 4 discusses the issues surrounding the design of resonant frequency control systems and provides simulation results of each resonance tuning system as well as experimental results for the RF plasma ignition system. Finally, Chapter 5 gives conclusions and outlines some future research directions.

1.4.2 Original Contributions

The primary contribution of this thesis is the development of systematic analysis and design methods for three resonant frequency control topologies. The first resonant frequency control method achieves resonant frequency tracking using an integrated self-oscillating feedback topology. A phase-lead compensator is used to compensate for the propagation delay in the RF generator and a signum type nonlinearity is used to achieve the amplitude limitation for sustained oscillation. The describing function method is employed for analysis and design of the self-oscillating resonance tracking system. The second method varies the excitation frequency to track the resonant

frequency of the system by seeking the frequency corresponding to a local maximum of the magnitude response. The third method varies a parameter in the resonant system to tune the resonant frequency to the excitation frequency by seeking the parameter value corresponding to a local maximum of the magnitude response.

Nonlinear models that accurately predict the performance of the resonant frequency control systems are developed. These developed models are then linearized to obtain more tractable linear time-invariant models that can be used for both analysis and design of the resonant frequency control systems. Based on the developed linear time-invariant models, specific guidelines for designing the resonant frequency control systems are also provided.

Two useful applications of these methods are presented. A novel RF plasma ignition system has been developed and tested on engine, and a control system based on a self-oscillating resonance tracking feedback topology has been implemented and tested. The proposed self-oscillating resonance tracking control method and the resonance seeking control method are applied through simulation of the ignition system to determine its potential effectiveness. Results from bench and on engine testing are also presented. These results are promising, and show that the system is a viable alternative to conventional ignition systems. The second example is based on the classical problem of tuning a dynamic vibration absorber to match the excitation frequency of a system. It is assumed that the absorber is a simple mass-spring-damper system with variable stiffness, and that the excitation frequency of the primary system is constant. Thus, the resonance tuning method is employed to tune the stiffness in the absorber to minimize amplitude of the primary system, and results are verified with simulation.

This thesis has generated one published work [48], and another paper is in preparation [49].

CHAPTER 2

Modeling

This chapter will present the models for the ignition system and dynamic vibration absorber, and a generic model for a resonator. Three control topologies that will be used for resonant frequency control are also proposed. The concept of resonance is also defined in this chapter for clarification.

2.1 Resonance

Scientist and engineers in various fields have used many definitions of resonance [6],[45],[47],[50],[51]. With such a diverse field of applications, it is difficult to reconcile these various concepts to one common definition of resonant frequency. Therefore, to prevent confusion the definition of resonant frequency will be fixed through two definitions. One definition will apply to second order systems, and the second to higher order resonant systems. Second order systems, such as the RLC circuit found in the RF plasma ignition system, have a single peak in the magnitude response very near their natural frequency. This can be seen in the second order system of the common form

$$H(s) = \frac{\omega_n^2}{s^2 + 2\zeta\omega_n s + \omega_n^2}, \tag{2.1}$$

where ω_n is the natural frequency of the system and ζ is the damping ratio. When such a system is lightly damped, the magnitude response $|H(j\omega)|$ has a peak near

$\omega = \omega_n$. Thus, the first definition of resonance is given as

Definition 2.1: *The resonant frequency, ω_r, of a second order system of the form where $0 < \zeta < 0.707$ is defined as ω_n [50],[52].*

For higher order systems with transfer function $H(s)$, the definition of resonance is not fixed since the properties of systems vary considerably. For example, a resonator may have more than one peak in its magnitude response. Thus the following definition of resonant frequency is given.

Definition 2.2: *The resonant frequency, ω_r, of a higher order system is defined as the frequency ω_r at which the magnitude response, $|H(j\omega_r)|$, reaches a local maximum [51].*

It should be noted that for second order systems this peak frequency occurs, more precisely, at $\omega_r = \omega_n\sqrt{1-2\zeta^2}$. Thus, if ζ is small, $\omega_n \approx \omega_n$. Therefore, the local maximum in $|H(j\omega)|$ occurs approximately at ω_n. Thus, for ζ sufficiently small, either definition can be applied to second order systems.

2.2 RF Plasma Ignition System

Prior to discharge, a spark plug can be modeled as a cylindrical capacitor with a very small capacitance value. Connecting an inductor in series with the spark plug forms a series RLC circuit, in which the resistor represents the losses in the physical components. By driving this RLC circuit with a suitable RF generator as shown in Figure 2.1 exactly at its resonant frequency, a very high RF voltage can be developed across the spark plug that results in an RF plasma torch. In this figure, R, L and C are the resistance, inductance and capacitance of the series RLC circuit; T, L_1, C_P, C_A and V form the RF generator; and D is the timing and gate driver circuit of the RF generator. The RF plasma torch generated this way can be used to ignite air-fuel mixtures in an internal combustion engine with appropriate ignition timing and duration.

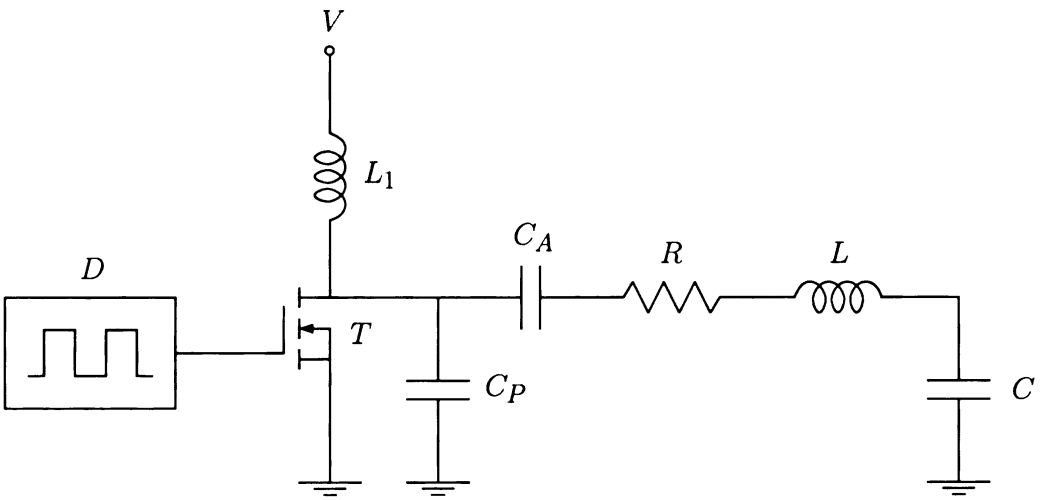

Figure 2.1. Proposed RF ignition system.

The gate driver and the RF generator can be modeled as

$$A(s) = Ke^{-s\tau}, \tag{2.2}$$

where τ is the propagation delay of the gate driver and RF generator combination and K is the gain of the RF generator. The load of the RF generator is a series RLC circuit with impedance

$$Z(s) = R + sL + \frac{1}{sC}. \tag{2.3}$$

The transfer function from the RLC circuit input voltage to the voltage across the capacitor is

$$H(s) = \frac{\frac{1}{LC}}{s^2 + \frac{R}{L}s + \frac{1}{LC}}. \tag{2.4}$$

Letting

$$\omega_n = \frac{1}{\sqrt{LC}} \tag{2.5}$$

be the angular resonant frequency and

$$\zeta = \frac{R}{2}\sqrt{\frac{C}{L}} \tag{2.6}$$

be the damping ratio of the RLC circuit, the transfer function $H(s)$ can be expressed as

$$H(s) = \frac{\omega_n^2}{s^2 + 2\zeta\omega_n s + \omega_n^2}. \tag{2.7}$$

Thus, the resonant frequency of this system can be defined by either method discussed above since there is only one peak in the magnitude response resulting from a single set of lightly damped complex conjugate poles.

Assuming that the input of the RLC circuit is of the form

$$v_1(t) = V_1 \cos(\omega t), \tag{2.8}$$

where V_1 is the amplitude and ω is the angular frequency of the input voltage, the voltage across the capacitor in the steady-state is

$$v_2(t) = |H(j\omega)|V_1 \cos[\omega t + \angle H(j\omega)]. \tag{2.9}$$

Thus, the amplitude of the voltage across the capacitor in the steady-state is

$$V_2 = |H(j\omega)|V_1. \tag{2.10}$$

If the angular frequency of the input is exactly equal to the angular resonant frequency of the RLC circuit, then the voltage V_2 becomes

$$V_2 = QV_1, \tag{2.11}$$

where

$$Q = \frac{1}{2\zeta} \tag{2.12}$$

is the quality factor of the RLC circuit. Thus, the amplitude of the voltage across the capacitor (spark plug before the breakdown) in the steady-state can be made sufficiently high to start a corona discharge if Q of the RLC circuit is sufficiently high. A Q factor of approximately 500 can be achieved by properly minimizing the losses in the RLC circuit. If, on the other hand, the input angular frequency of the RLC circuit is slightly different (even only 1%) from the resonant frequency of the RLC circuit, then the voltage across the capacitor will not be sufficient enough to start a corona discharge. Hence, even if the *RLC* circuit is driven initially at its resonance, its resonant frequency or driving frequency may shift in time due to environmental

changes, reducing the achievable high voltage across the spark plug drastically and rendering the ignition system completely inadequate. This mandates the use of a control system that tracks the resonant frequency of the RLC load connected to the RF generator and drives it at its resonant frequency despite environmental disturbances. For control purposes the current through the load is used for feedback since it can be easily measured. The transfer function $G(s)$ is the transfer function of the RLC circuit from its voltage input to the current through it and is given by

$$G(s) = \frac{\gamma s}{s^2 + 2\zeta\omega_n s + \omega_n^2}, \tag{2.13}$$

where $\gamma = L/C$.

The nominal values for the RLC circuit are $R = 5.80\ \Omega$, $L = 14.86 \times 10^{-6}$ H, $C = 10.10 \times 10^{-12}$ F. Thus, the nominal values of ω_0, ζ and Q are $\omega_{0n} = 81.63 \times 10^6$ rad/s, $\zeta_n = 2.39 \times 10^{-3}$ and $Q_n = 209.13$. The gain of the RF generator is $K = 20.00$ and the propagation delay of the RF generator and its gate driver is $\tau = 43.00 \times 10^{-9}$ s. Due to the environmental disturbances, L or C values can change within 5% of their respective nominal values so that the angular resonant frequency of the RLC circuit can take any value in the interval $[77.74 \times 10^6,\ 85.92 \times 10^6]$ rad/s.

2.3 Vibration Absorber

The classical tuned dynamic vibration absorber problem is to design an absorber such that when attached to a primary system, it will minimize its vibration due to excitation at a particular frequency. This is useful for systems where resonance of the primary system without an absorber is a problem. The primary system is assumed to be an MSD system, and the absorber will be another MSD mounted directly on the mass of the primary system. Figure 2.2 shows a diagram of a standard absorber. In this diagram, k_a and k_p are spring constants, c_a and c_p are damping constants, and m_a and m_p are masses of the absorber and primary system, respectively. x_a is the

displacement of the absorber relative to the primary mass, and x_p is the displacement of the primary mass relative to its stationary mount, and $u(t)$ represents a force acting on the primary mass that is assumed to be of the form $u(t) = F_0 \sin \omega_0 t$.

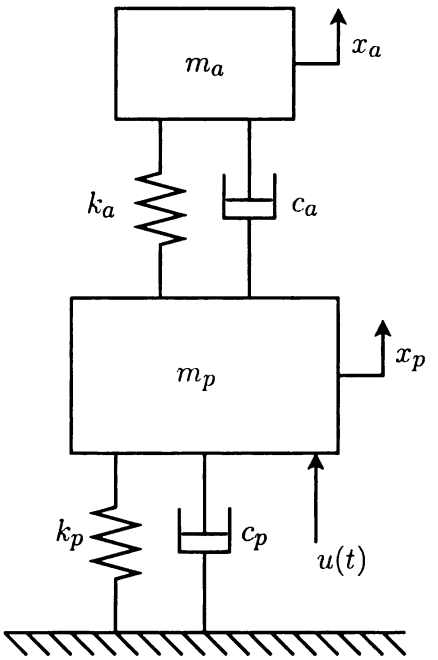

Figure 2.2. Model of dynamic vibration absorber.

Thus, the goal is to minimize the vibration in the primary mass. This requires the system be excited at the mode corresponding to the resonant frequency of the absorbing MSD system. The following state space equation governs the dynamics of the vibration absorber system,

$$\begin{pmatrix} \dot{x}_1 \\ \dot{x}_2 \\ \dot{x}_3 \\ \dot{x}_4 \end{pmatrix} = \begin{bmatrix} 0 & 1 & 0 & 0 \\ -\frac{k_p}{m_p} & -\frac{c_p}{m_p} & \frac{k_a}{m_p} & \frac{c_a}{m_p} \\ 0 & 0 & 0 & 1 \\ \frac{k_p}{m_p} & \frac{c_p}{m_p} & -\left(\frac{1}{m_p}+\frac{1}{m_a}\right)k_a & -\left(\frac{1}{m_p}+\frac{1}{m_a}\right)c_a \end{bmatrix} \begin{pmatrix} x_1 \\ x_2 \\ x_3 \\ x_4 \end{pmatrix} + \begin{pmatrix} 0 \\ \frac{1}{m_p} \\ 0 \\ \frac{1}{-m_p} \end{pmatrix} u(t), \tag{2.14}$$

where $x_1 = x_p$ and $x_3 = x_a - x_p$. It is assumed that the position x_p of the original mass is available for feedback. The forced mass-spring-damper example selection was chosen to have mass $m_p = 0.1$ kg, spring stiffness $k_p = 1000$ N/m, and a damping rate of $c_p = 0.09$ Ns/m, and the absorber was chosen with mass $m_p = 0.02$ kg, a nominal spring stiffness $k_a = 200$ N/m, and a damping value $c_a = 0.02$ Ns/m. The design of the absorber is tailored to the natural frequency of the primary system, $w_{n1} = 100$ rad/s. Figure 2.3 shows a bode plot for the primary MSD system with and without a vibration absorber. With the absorber, it is clear that the magnitude response of the primary system is minimized at the resonant frequency, which occurs at about 100 rad/sec.

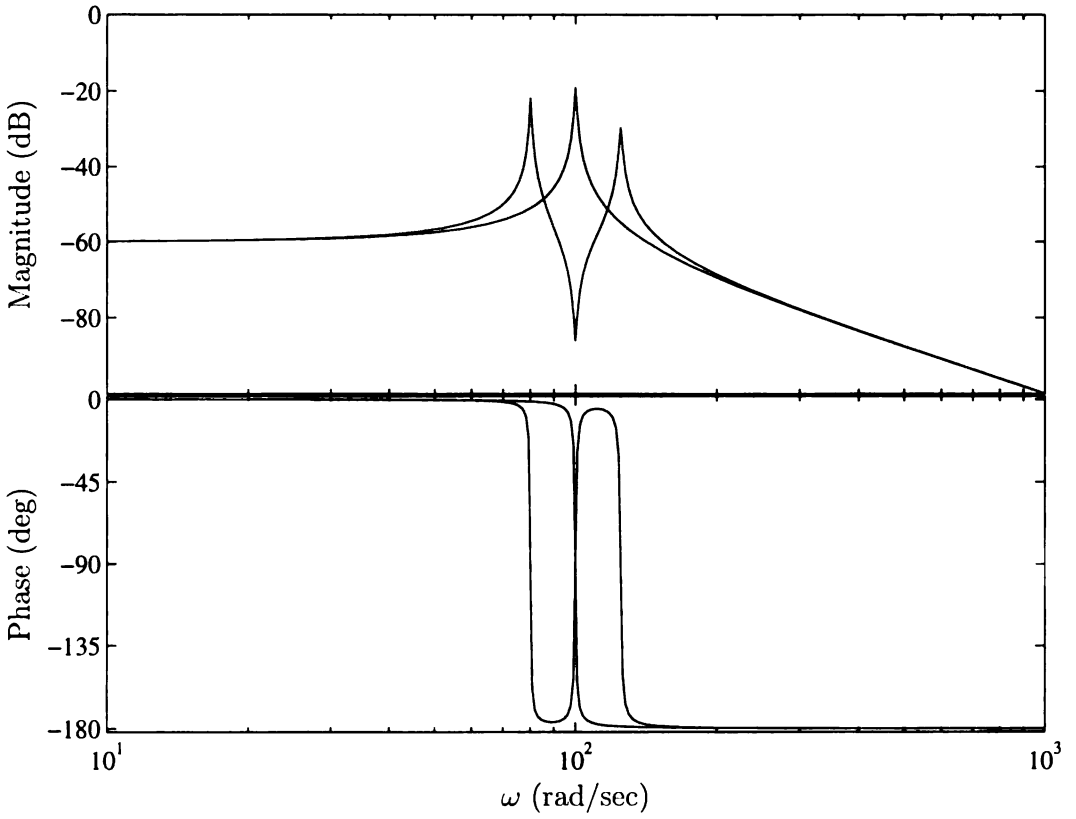

Figure 2.3. Bode plot of MSD with and without dynamic vibration absorber.

If the excitation frequency of the primary system or the parameters of the absorber

are disturbed, the absorber must be retuned for the magnitude response of the primary system to be minimized. To accomplish this, the parameter k_a is considered to be a variable stiffness and it is further assumed that this stiffness can be actively adjusted [40]-[44]. Controlling this value allows the absorber to be dynamically tuned to account for changes in the resonant frequency or excitation frequency.

2.4 Resonator

Based on the above applications, it is desirable to formulate the resonant frequency control problems with a generic resonator model. Thus, based on the intended applications, a resonator model is proposed in Figure 2.4. In this figure, $v(t)$ and $y(t)$ are the system input and output, respectively, while $H(s, \xi, \kappa)$ is the resonant system, where $\xi = [\xi_1 \cdots \xi_n]^T$ is a adjustable structural parameter of the system, and $\kappa = [\kappa_1 \cdots \kappa_n]^T$ is a structural parameter of the system which may drift due to disturbances discussed above but which cannot be adjusted. These parameters are assumed to be constant but unknown, with nominally known values.

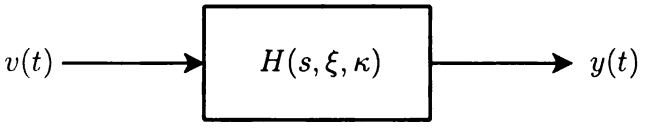

Figure 2.4. Model of resonant system.

2.5 Self-Oscillating Resonance Tracking Control

This section presents the topology and modeling of a self-oscillating resonance frequency tracking control system as a solution to resonating second-order systems with a time delay. The RF plasma ignition system can be modeled as such, with the RLC circuit being modeled a second-order system, and the inherent time delay in the gate driver and RF amplifier considered to be significant.

Motivated by the previous discussion, the following self-oscillating resonance frequency tracking system shown in Figure 2.5 is considered. In this figure, the transfer function $A(s)$ represents the driver system and is assumed to be in the form

$$A(s) = Ke^{-s\tau}, \tag{2.15}$$

where τ is the time delay in the driver system and K is the gain of the driving system; $G(s)$ is the transfer function of the resonant system, given by

$$G(s) = \frac{\gamma s}{s^2 + 2\zeta\omega_n s + \omega_n^2}. \tag{2.16}$$

The transfer function $C(s)$ is a phase-lead type compensator to be designed to compensate for the phase delay in the driving system and is assumed to be in the form

$$C(s) = 1 + \eta s, \tag{2.17}$$

where η is a design parameter, and the static nonlinearity $\varphi(u)$ is a signum type nonlinearity to achieve amplitude limiting mechanism for self-oscillation and is assumed to be of the form

$$\varphi(u) = \beta \operatorname{sgn}(u), \tag{2.18}$$

where sgn is the standard signum function and β is a design parameter. Moreover, $x(t)$ is the input resonant system, $y(t)$ is the output of the resonant system, $u(t)$ is the input of the signum nonlinearity, $v(t)$ is the output of the signum nonlinearity and the negative feedback sign is used for the sake of convention.

The parameters of the resonant system are assumed to be constant but unknown with known nominal values to take into account the effect of environmental disturbances on the load. Moreover, the output of the resonant system is assumed to be available for feedback purposes.

With the above assumptions, the self-oscillating resonance tracking problem is to design the compensator $C(s)$ and the signum nonlinearity $\varphi(u)$ to start and sustain a self-oscillation with angular frequency sufficiently close to the nominally known resonant frequency of the resonant system despite inherent disturbances.

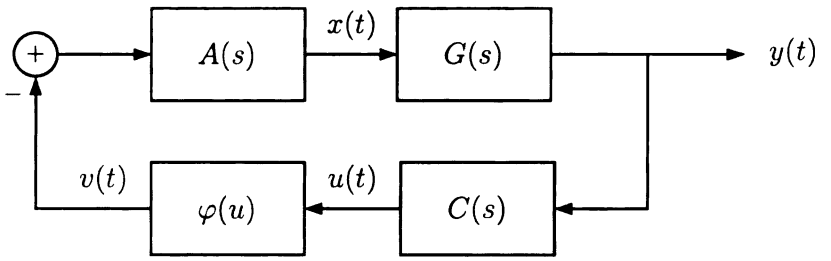

Figure 2.5. Self-oscillating resonance tracking system model.

2.6 Resonance Seeking Control

In this section, the model for resonance seeking control is presented. This control method is a form of adaptive control which seeks the excitation frequency corresponding to a local maximum in the magnitude response of a system. Thus, the proposed control system is designed to excite systems at their resonant frequency, as given in the first definition above. Unlike the self-oscillating resonance tracking control topologies, the resonant system is excited by a constant amplitude, variable frequency sinusoidal signal source. The sinusoidal input signal $v(t)$ to the resonant system with transfer function $H(s)$ in the steady state results in the sinusoidal output, $y(t)$, the magnitude of which should be maximized. Thus the input is assumed to take the form

$$v(t) = V \sin(\omega_s t + \theta) \tag{2.19}$$

where V is the amplitude of the input, ω_s is the angular driving frequency, and θ is the phase angle. Thus, at steady state, the output $y(t)$, is

$$y(t) = V|H(j\omega_s)| \sin[\omega_s t + \theta + \angle H(j\omega_s)]. \tag{2.20}$$

The magnitude $M(\omega_s)$ is defined as the average of the absolute value of $y(t)$, and is given by

$$M(\omega_s) = \frac{2}{\pi} V|H(j\omega_s)|. \tag{2.21}$$

The magnitude $M(\omega_s)$ reaches a local maximum when $\omega_s = \omega_r$ by the second definition of resonant frequency given above. Thus, resonance occurs when

$$M'(\omega_r) = 0 \tag{2.22}$$

and

$$M''(\omega_r) < 0. \tag{2.23}$$

As discussed previously, ω_s can be determined nominally, but may deviate from ω_r causing degradation in performance of the system. Thus, a closed loop system is used to enforce the condition that $\omega_s \simeq \omega_r$.

For the proposed control system, it is assumed that the output of the resonant system is measurable for feedback purposes. The control system requires access to $M'(\omega_s)$, in order to properly regulate ω_s. This derivative cannot be measured directly, so a method for estimating it is developed. To accomplish this estimation, a small sinusoidal perturbation is added to the source frequency ω_s. The average magnitude response with respect to this perturbation is then estimated.

To demonstrate how this is accomplished, Figure 2.6 presents the proposed control system. In this figure, $H(s)$ is the transfer function of the system that shall be excited at its resonant frequency. The absolute value of the signal $y(t)$ is taken, resulting in the signal $m(t)$. The average of $m(t)$ thus is $M(\omega_s)$. The multiplication operator and filter $F(s)$ perform synchronous demodulation to estimate the required derivative $M'(\omega_s)$. The lower section of the system represents the variable frequency oscillator, with amplitude V and instantaneous angular driving frequency $\omega_s(t)$, as well as the nominal angular center frequency ω_0 and the small perturbation frequency $\varepsilon \cos(\sigma t)$. The signals $x(t)$ and $z(t)$ represent the input and output, respectively, of the filter $F(s)$. The controlled phase of the variable frequency oscillator is represented by $\theta(t)$, and the k_ω is the angular frequency feedback gain.

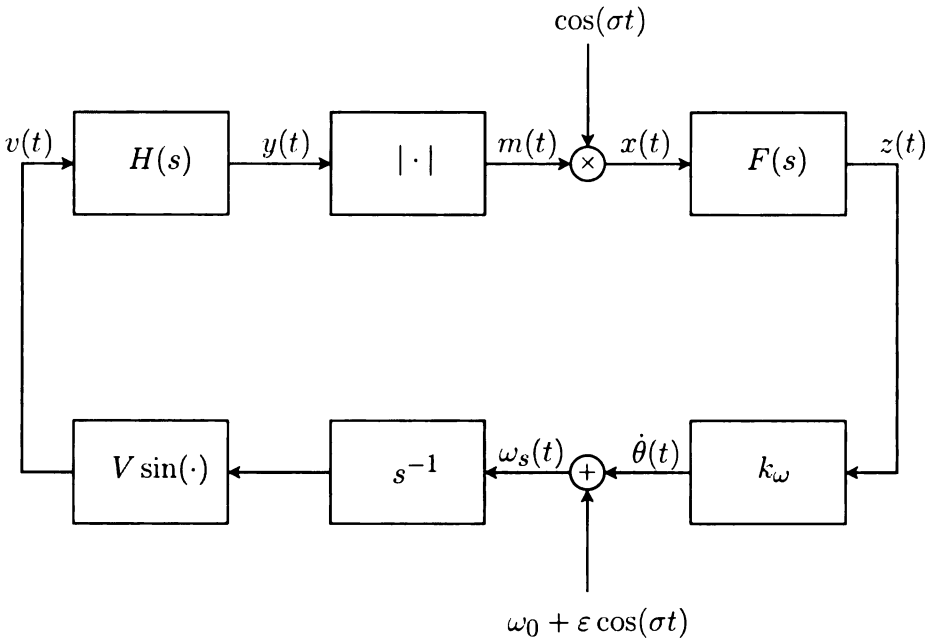

Figure 2.6. Model of resonance seeking control system.

2.7 Resonance Tuning Control

In this section, the model for resonance tuning control is presented. This control method is a form of adaptive control which tunes a system parameter value ξ corresponding to local maxima in the magnitude response of the resonant system. Thus, the proposed control system is designed to excite systems at their resonance frequency as defined in Definition 1 by tuning the resonator to the excitation frequency rather than seeking the resonant frequency of the resonator. The system is excited by a sinusoidal signal source $v(t)$, with constant amplitude V, and constant angular frequency ω_0. The sinusoidal input signal $v(t)$ to system $H(s)$ results in the sinusoidal output, $y(t)$, the magnitude of which should be maximized. Further, a structural parameter, ξ, of the system is adjusted by a second input signal ξ_s, unlike the resonance seeking system. This signal ξ_s is assumed to slowly time varying. Since the control system will tune this parameter to achieve resonant frequency control, the transfer function for the resonant system $H(s)$ will be denoted $H(s, \xi)$. An example of such a system

is the dynamic vibration absorber, there the adjustable parameter ξ is the variable stiffness k_a. The output the system at steady state therefore assumes the form

$$y(t) = V|H[j\omega_0, \xi_s(t)]| \sin\{\omega_0 t + \angle H[j\omega_s, \xi_s(t)]\} \tag{2.24}$$

The magnitude $M_{\omega_0}(\xi_s)$ is defined as the average of the absolute value of $y(t)$, and is given by

$$M_{\omega_0}(\xi_s) = \frac{2}{\pi} V|H(j\omega_0, \xi_s)| \tag{2.25}$$

The magnitude $M_{\omega_0}(\xi_s)$ reaches a local maximum when $\xi_s = \xi_r$, where ξ_r is the parameter value corresponding the the maximum value of $|H(j\omega_0, \xi)|$. Therefore, considering the second definition of resonant frequency above, but applying it to a structural parameter rather than a frequency, resonance occurs when

$$M'_{\omega_0}(\xi_r) = 0 \tag{2.26}$$

and

$$M''_{\omega_0}(\xi_r) < 0. \tag{2.27}$$

As discussed previously, ξ_s can be determined nominally, but may deviate from ξ_r causing a degradation in performance of the system. Thus, a closed loop system is used to enforce the condition that $\xi_s \simeq \xi_r$.

For the proposed control system, it is assumed that the output of the system is measurable for feedback purposes. The control system requires access to $M'_{\omega_0}(\xi_s)$, in order to properly regulate ξ_s. This derivative cannot be measured directly, so a method for estimating it is developed. To accomplish this measurement, a small sinusoidal perturbation is added to the source signal ξ_s. The average magnitude response with respect to this perturbation is then estimated.

To demonstrate how this is accomplished, Figure 2.7 presents the proposed control system. In this figure, $H(s, \xi)$ is the transfer function of the system that shall be excited at resonance. The absolute value taken the signal $y(t)$ is taken, yielding

the signal $m(t)$. The average of $m(t)$ thus becomes $M_{\omega_0}(\xi_s)$, the scaled magnitude response of the resonant system at steady state. The multiplication operator and filter $F(s)$ perform synchronous demodulation to estimate the required derivative $M'_{\omega_0}(\xi_s)$. The signals $x(t)$ and $z(t)$ represent the input and output, respectively, of the filter $F(s)$. The lower section of the system provides the parameter value feedback loop gain k_ξ, perturbation frequency $\varepsilon\cos(\sigma t)$, and addition of initial parameter value ξ_0 to yield the instantaneous parameter value $\xi_s(t)$.

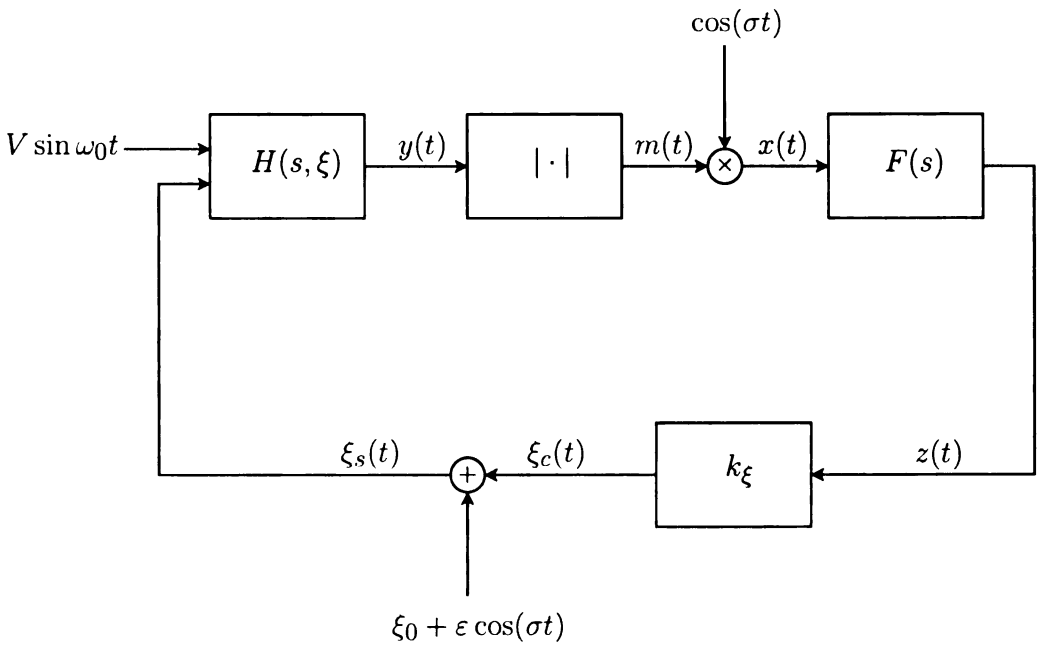

Figure 2.7. Model of resonance tuning control system.

CHAPTER 3

Analysis

In this section, the resonant frequency control models developed in Chapter 2 are considered and analysis methods are developed. To take into account disturbances that affect the resonant frequency of the systems, the uncontrolled parameters of the resonant system are assumed to be constant but unknown. Three main resonant frequency control systems are analyzed. First, self-oscillating resonance tracking control is analyzed for second order systems with time delay. Next, resonance seeking and resonance tuning control are developed. Nonlinear and linear models for both resonance seeking and resonance tuning control systems are also presented to aid in the design process.

3.1 Self-Oscillating Resonance Tracking Control

Consider the self-oscillating resonance tracking system shown in Figure 2.5. The method of describing function is used to facilitate analysis and design of this system. Since the resonant system is assumed to have sufficiently high quality factor, the output is practically equal to the first harmonic of the signal in the loop. Thus, the use of the describing function method is justified.

Assuming that the signal $y(t)$ in the steady-state is essentially of the form

$$y(t) = Y\cos(\omega t), \tag{3.1}$$

it follows that the signal $u(t)$ in the steady-state is given by

$$u(t) = |C(j\omega)|Y\cos[\omega t + \angle C(j\omega)]. \tag{3.2}$$

Thus, the signal $v(t)$ in the steady-state can be expressed as

$$v(t) = N[|C(j\omega)|Y]|C(j\omega)|Y\cos[\omega t + \angle C(j\omega)] + e(t), \tag{3.3}$$

where $e(t)$ is the sum of higher order harmonics and $N(\alpha)$ is the describing function (equivalent gain) of the signum nonlinearity given by

$$N(\alpha) = \frac{4\beta}{\pi\alpha}. \tag{3.4}$$

Then, the signal $x(t)$ in the steady-state can be expressed as

$$\begin{aligned} x(t) = |A(j\omega)|N[|C(j\omega)|Y]|C(j\omega)|Y\cos[\omega t + \angle A(j\omega) + \angle C(j\omega) + \pi] \\ -a(t) * e(t), \end{aligned} \tag{3.5}$$

where $a(t)$ is the inverse Laplace transform of $A(s)$. Thus, the signal $y(t)$ in the steady-state turns out to be

$$\begin{aligned} y(t) = |G(j\omega)||A(j\omega)|N[|C(j\omega)|Y]|C(j\omega)|Y\cos[\omega t + \angle G(j\omega) \\ +\angle A(j\omega) + \angle C(j\omega) + \pi] - g(t) * a(t) * e(t), \end{aligned} \tag{3.6}$$

where $g(t)$ is the inverse Laplace transform of $G(s)$. Hence, assuming that the term $g(t) * a(t) * e(t)$ is negligibly small due to filtering in $G(s)$, it follows that

$$1 + G(j\omega)A(j\omega)N[|C(j\omega)|Y]C(j\omega) = 0, \tag{3.7}$$

which is the (first-order) harmonic balance equation. Equivalently,

$$|G(j\omega)||A(j\omega)|N[|C(j\omega)|Y]|C(j\omega)|\cos[\angle G(j\omega) + \angle A(j\omega) + \angle C(j\omega)] = -1 \tag{3.8}$$

and

$$|G(j\omega)||A(j\omega)|N[|C(j\omega)|Y]|C(j\omega)|\sin[\angle G(j\omega) + \angle A(j\omega) + \angle C(j\omega)] = 0. \tag{3.9}$$

Moreover, since $|A(j\omega)|N[|C(j\omega)|Y]|C(j\omega)| \neq 0$, equation (3.9) can be simplified as

$$|G(j\omega)|\sin[\angle G(j\omega) + \angle A(j\omega) + \angle C(j\omega)] = 0. \tag{3.10}$$

This equation is independent of Y and thus can be easily solved for ω to determine the estimated angular frequency of oscillation. Once the estimated angular frequency of oscillation is determined, the estimated amplitude of oscillation can be determined by solving equation (3.8) for Y.

It follows from equation (3.10) that the estimated angular frequency of oscillation ω is equal to the angular resonant frequency of the resonant system independent of environmental disturbances provided that

$$\angle A(j\omega) + \angle C(j\omega) \equiv 0, \ \text{mod}\ \pi. \tag{3.11}$$

However, it is impossible to satisfy this condition by a finite dimensional transfer function $C(s)$. Nevertheless, with the assumed simple form of $C(s)$, the phase-lag introduced by the driving system can be compensated at least for the nominal angular frequency ω_{n0}. Noting that the phase of the transfer function $A(j\omega)$ is

$$\angle A(j\omega) = -\omega\tau, \tag{3.12}$$

the design parameter η in the transfer function $C(s)$ is selected to satisfy

$$\angle C(j\omega_{n0}) + \angle A(j\omega_{n0}) \equiv 0, \ \text{mod}\ \pi. \tag{3.13}$$

Thus, it turns out that

$$\eta = \frac{1}{\omega_{n0}}\tan(\omega_{n0}\tau). \tag{3.14}$$

With this choice, it follows from equation (3.10) that

$$|G(j\omega)|\sin[\angle G(j\omega)] \approx 0, \tag{3.15}$$

provided that

$$\angle C(j\omega) + \angle A(j\omega) \approx 0, \ \text{mod}\ \pi. \tag{3.16}$$

Hence, the angular oscillation frequency ω is approximately equal to the angular resonant frequency ω_n of the resonant system provided that the above condition is satisfied. Clearly, equation (3.10) can be solved numerically to determine a better estimate for the angular oscillation frequency.

Having determined the angular oscillation frequency ω, equation (3.8) can be solved numerically to estimate the amplitude of the oscillation Y. An analytical estimate for the amplitude of the oscillation can be also obtained by using the approximation $\omega \approx \omega_n$. With this assumption, it follows from equation (3.8) that

$$N[|C(j\omega_n)|Y] = -\frac{2\zeta\omega_n}{\gamma K\sqrt{1+\eta^2\omega^2}} \tag{3.17}$$

when $\omega_n\tau \in (-\pi/2, +\pi/2)$, $\mathrm{mod}\,(2\pi)$ and

$$N[|C(j\omega_n)|Y] = +\frac{2\zeta\omega_n}{\gamma K\sqrt{1+\eta^2\omega^2}} \tag{3.18}$$

when $\omega_n\tau \in (+\pi/2, +3\pi/2)$, $\mathrm{mod}\,(2\pi)$. Hence, the amplitude of the oscillation is given by

$$Y = \frac{2\gamma K\beta}{\pi\zeta\omega_n}\,\mathrm{sgn}\,(N[|C(j\omega_n)|Y]). \tag{3.19}$$

Note further that the parameter β turns out to be

$$\beta = \frac{\pi\zeta\omega_n Y}{2\gamma K}\,\mathrm{sgn}\,(N[|C(j\omega_n)|Y]). \tag{3.20}$$

3.2 Resonance Seeking Control

This section details the development of a nonlinear model that can accurately represent the resonance seeking control system. For additional use in system design, a simple linear time-invariant model is also developed.

Consider the system model presented in Figure 2.6. The angular frequency of the driving signal, $\omega_s(t)$, can be written as

$$\omega_s(t) = \omega_0 + \dot{\theta}(t) + \varepsilon\cos(\sigma t), \tag{3.21}$$

where

$$\dot{\theta}(t) = k_\omega z(t). \tag{3.22}$$

It follows then that the driving signal can be expressed as

$$v(t) = V \sin[\omega_0 t + \phi_V(t)], \tag{3.23}$$

where

$$\phi_V(t) = \theta(t) + \frac{\varepsilon}{\sigma} \sin(\sigma t). \tag{3.24}$$

The signal $\theta(t)$ is assumed to be slowly time varying, and σ is assumed to be sufficiently small relative to ω_0, resulting in the following approximation:

$$y(t) = Y \sin[\omega_0 t + \phi_Y(t)] \tag{3.25}$$

where

$$Y = V|H[j\omega_s(t)]|, \tag{3.26}$$

and

$$\phi_Y(t) = \theta(t) + \frac{\varepsilon}{\sigma} \sin(\sigma t) + \angle H[j\omega_s(t)]. \tag{3.27}$$

It follows that the instantaneous magnitude is

$$m(t) = |y(t)| \tag{3.28}$$

which can also be written as

$$\begin{aligned} m(t) &= y(t)\text{sgn}[y(t)] \\ &= Y \sin[\omega_0 t + \phi_Y(t)]\text{sgn}\{\sin[\omega_0 t + \phi_Y(t)]\} \end{aligned} \tag{3.29}$$

Using the following Fourier series expansion,

$$\text{sgn}[\sin(\omega x)] = \frac{4}{\pi} \sum_{n \text{ odd}}^{\infty} \frac{1}{n} \sin(\omega n x), \tag{3.30}$$

It can easily be shown that

$$\text{sgn}[y(t)] = \frac{4}{\pi} \sum_{n \text{ odd}}^{\infty} \frac{1}{n} \sin[\omega_0 n t + n\phi_Y(t)]. \tag{3.31}$$

Therefore, from equation (3.29) it follows that

$$m(t) = \frac{4Y}{\pi} \sin[\omega_0 t + \phi_Y(t)] \sum_{n \text{ odd}}^{\infty} \frac{1}{n} \sin[\omega_0 n t + n\phi_Y(t)]. \tag{3.32}$$

Applying the trigonometric identity $\sin^2(x) = \frac{1}{2}[1 - \cos(2x)]$ yields

$$m(t) = \frac{2Y}{\pi}\{1 - \cos[2\omega_0 t + 2\phi_Y(t)]\} + p(t), \tag{3.33}$$

where $p(t)$ represents higher order terms. Noting that

$$M[\omega_s(t)] = \frac{2Y}{\pi}, \tag{3.34}$$

it follows that

$$m(t) = M[\omega_s(t)]\{1 - \cos[2\omega_0 t + 2\phi_Y(t)]\} + p(t) \tag{3.35}$$

Assuming ε is sufficiently small, $M[\omega_s(t)]$ is expanded into its Taylor series about $\omega(t) = \omega_0 + \dot{\theta}(t)$. $M[\omega_s(t)]$ is therefore approximated as

$$M[\omega_s(t)] = M[\omega(t)] + M'[\omega(t)]\varepsilon \cos(\sigma t) \tag{3.36}$$

It follows then, from equation (3.35), that

$$m(t) = \{M[\omega(t)] + M'[\omega(t)]\varepsilon \cos[\sigma(t)]\}\{1 - \cos[2\omega_0 t + 2\phi_Y(t)]\} + p(t)$$

An expression has now been obtained that contains the derivative of the magnitude response with respect to frequency. To isolate this term, the signal is multiplied by $\cos(\sigma t)$. So from Figure 2.6,

$$x(t) = m(t)\cos(\sigma t) \tag{3.37}$$

With some trigonometric manipulation, $x(t)$ can be written as

$$x(t) = \frac{\varepsilon}{2} M'[\omega(t)] + q(t) \tag{3.38}$$

where the term $q(t)$ includes higher frequency components around σ, 2σ, $2\omega_0 - \sigma$, $2\omega_0 + \sigma$, $(n-1)w_0 + \sigma$, $(n-1)w_0 + \sigma$, $(n+1)w_0 + \sigma$, and $(n+1)w_0 - \sigma$. Passing

the signal $x(t)$ through the low pass filter $F(s)$ attenuates these signals, so assuming these signals are entirely eliminated,

$$z(t) = \frac{\varepsilon}{2} f(t) * M'[\omega(t)], \tag{3.39}$$

where $f(t)$ is the impulse response of the filter $F(s)$, and $*$ is the convolution operation. It follows from (3.22) that

$$\dot{\theta}(t) = \frac{k_\omega \varepsilon}{2} f(t) * M'[\omega(t)]. \tag{3.40}$$

Considering that $\dot{\theta} = \omega(t) - \omega_0$, the equation becomes

$$\omega(t) - \omega_0 = \frac{k_\omega \varepsilon}{2} f(t) * M'[\omega(t)], \tag{3.41}$$

where

$$\omega(t) = \omega_s(t) - \varepsilon \cos(\sigma t). \tag{3.42}$$

This equation is an approximation of the dynamic behavior of the frequency in the resonance seeking control system. If the assumptions stated above are satisfied, simulation indicates that this nonlinear equation accurately describes the dynamics of the proposed system. Based on this equation, and assuming that the closed loop system is stable, the steady state value ω_{ss} of $\omega(t)$ must satisfy

$$\omega_{ss} - \omega_0 = \frac{k_\omega \varepsilon}{2} F(0) * M'[\omega_{ss}]. \tag{3.43}$$

Therefore, if $F(s)$ contains at least one integrator, $M'[\omega(t)]$ will approach a steady state value of zero. Thus the instantaneous frequency $\omega(t)$ asymptotically approaches the resonant frequency of the resonator ω_r, or similarly the driving frequency $\omega_s(t)$ asymptotically approaches $\omega_r + \varepsilon \cos(\sigma t)$. Thus, to ensure that $\omega_s(t)$ at steady state is very close to the resonant frequency ω_r, ε should be chosen to be sufficiently small.

For design purposes, however, a simplified linear time-invariant model is desirable. To accomplish this, the nonlinear equation (3.41) can be linearized about its nominal frequency ω_0, or for a more useful linearization, about its nominal system parameters

ω_0 and κ_0. To linearize about ω_0, take $\delta\omega(t) = \omega(t) - \omega_0$, and expand $M'[\omega_0 + \delta\omega(t)]$ into its Taylor series. Retain only the first two terms to give

$$\delta\omega(t) = \frac{k_\omega \varepsilon}{2} f(t) * [M'(\omega_0) + M''(\omega_0)\delta\omega(t)]. \tag{3.44}$$

The linearization from this expansion results in a less straightforward final form since $M'(\omega_0)$ still depends on the uncontrollable system parameter κ. This leads to linearization about the nominal frequency ω_0 and nominal resonant system parameter κ_0. Take $\delta\kappa = \kappa - \kappa_0$, and denote $M(\omega)$ as $M(\omega, \kappa)$ since it is also dependent on the system parameter κ. Then $M'[\omega_0 + \delta\omega(t), \kappa_0 + \delta\kappa]$ is expanded into its Taylor series and higher order terms are ignored, yielding

$$\delta\omega(t) = \frac{k_\omega \varepsilon}{2} f(t) * \left[M'(\omega_0, \kappa_0) + \frac{\partial}{\partial\omega} M'(\omega, \kappa)\Big|_{\substack{\omega=\omega_0 \\ \kappa=\kappa_0}} \delta\omega(t) + \frac{\partial}{\partial\kappa} M'(\omega, \kappa)\Big|_{\substack{\omega=\omega_0 \\ \kappa=\kappa_0}} \delta\kappa \right]. \tag{3.45}$$

Note that the derivatives of M in this equation are all dependant on nominal values and that $M'(\omega_0, \kappa_0) = 0$. Thus the linearized equations can be written as

$$\delta\omega(t) = k f(t) * [\delta\omega_r - \delta\omega(t)]. \tag{3.46}$$

where

$$k = -\frac{k_\omega \varepsilon}{2} \frac{\partial^2}{\partial\omega^2} M(\omega, \kappa)\Big|_{\substack{\omega=\omega_0 \\ \kappa=\kappa_0}} \tag{3.47}$$

and

$$\delta\omega_r = -\frac{\frac{\partial^2}{\partial\kappa\partial\omega} M(\omega, \kappa)\Big|_{\substack{\omega=\omega_0 \\ \kappa=\kappa_0}}}{\frac{\partial^2}{\partial\omega^2} M(\omega, \kappa)\Big|_{\substack{\omega=\omega_0 \\ \kappa=\kappa_0}}} \delta\kappa, \tag{3.48}$$

where $\delta\omega_r$ is the deviation of the resonant frequency from the nominal value ω_0. Lastly, from equation (3.42) it can be seen that

$$\delta\omega_s(t) = \delta\omega(t) + \varepsilon\cos(\sigma t). \tag{3.49}$$

To further demonstrate these equations, a block diagram is presented in Figure 3.1 that represents the linearized model in equation (3.46). Thus, the closed loop resonance seeking control system behavior can be analyzed with standard linear system techniques. Simulation results indicate that this linear time-invariant model is quite accurate, given the above assumptions.

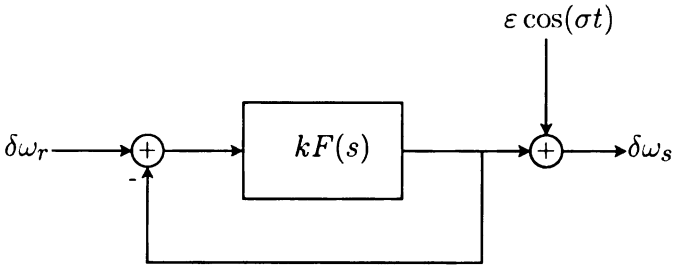

Figure 3.1. Simplified linear model of resonance seeking control system.

Also, it is important to note that $F(s)$ plays a primary role in the resonance seeking control system. It can be easily seen that the linear system of equation 3.46 is stable if all the roots of the characteristic equation $1 + kF(s) = 0$ have negative real parts. Thus, the original nonlinear system shown in Figure 2.6 is locally asymptotically stable if this condition is satisfied.

3.3 Resonance Tuning Control

This section details the development of a nonlinear model that can accurately represent the resonance tuning control system. As in the last section, for additional use in system design, a simple linear time-invariant model is also developed.

Consider the system model presented in Figure 2.7. The parameter ξ of $H(s)$, is tuned to adapt the resonant frequency of the system to the excitation frequency. Thus, the input signal $\xi_s(t)$ which controls this parameter can be written as

$$\xi_s(t) = \xi_0 + \xi_c(t) + \varepsilon\cos(\sigma t), \tag{3.50}$$

where

$$\xi_c(t) = k_\xi z(t). \tag{3.51}$$

The driving signal can be expressed as

$$v(t) = V \sin(\omega_0 t), \tag{3.52}$$

The signal $\xi_c(t)$ is assumed to be slowly time varying, and σ is assumed to be sufficiently small relative to ξ_0, resulting in the following approximation:

$$y(t) = Y \sin(\omega_0 t + \phi_Y) \tag{3.53}$$

where

$$Y = V|H[j\omega_0, \xi_s(t)]|, \tag{3.54}$$

and

$$\phi_Y = \angle H[j\omega_0, \xi_s(t)] \tag{3.55}$$

It follows that the instantaneous magnitude is

$$m(t) = |y(t)| \tag{3.56}$$

which can also be written as

$$m(t) = y(t)\text{sgn}[y(t)]. \tag{3.57}$$

Recalling equation (3.30), it follows that

$$\text{sgn}[y(t)] = \frac{4}{\pi} \sum_{n=1,3,5,\ldots}^{\infty} \frac{1}{n} \sin(\omega_0 n t + n\phi_Y(t)). \tag{3.58}$$

Thus, the signal $m(t)$, by equation (3.53), becomes

$$m(t) = \frac{4Y}{\pi} \sin[\omega_0 t + \phi_Y(t)] \sum_{n\,\text{odd}}^{\infty} \frac{1}{n} \sin[\omega_0 n t + n\phi_Y(t)]. \tag{3.59}$$

Applying the trigonometric identity $\sin^2(x) = \frac{1}{2}[1 - \cos(2x)]$ yields

$$m(t) = \frac{2Y}{\pi}\{1 - \cos[2\omega_0 t + 2\phi_Y(t)]\} + p(t) \tag{3.60}$$

where $p(t)$ represents higher order terms. Noting that

$$M_{\omega_0}[\xi_s(t)] = \frac{2Y}{\pi}, \tag{3.61}$$

it follows that

$$m(t) = M_{\omega_0}[\xi_s(t)]\{1 - \cos[2\omega_0 t + 2\phi_Y(t)]\} + p(t) \tag{3.62}$$

Assuming ε is sufficiently small, $M_{\omega_0}[\xi_s(t)]$ is expanded into its Taylor series about $\xi(t) = \xi_0 + \xi_c(t)$. $M_{\omega_0}[\xi_s(t)]$ is therefore approximated as

$$M_{\omega_0}[\xi_s(t)] = M_{\omega_0}[\xi(t)] + M'_{\omega_0}[\xi(t)]\varepsilon\cos(\sigma(t)). \tag{3.63}$$

It then follows that equation (3.62) becomes

$$\begin{aligned} m(t) = & \left\{M_{\omega_0}[\xi(t)] + M'_{\omega_0}[\xi(t)]\varepsilon\cos[\sigma(t)]\right\}\{1 - \cos[2\omega_0 t + 2\phi_Y(t)]\} \\ & + p(t) \end{aligned} \tag{3.64}$$

An expression has now been obtained that contains the derivative of the magnitude response with respect to the adjustable parameter. To isolate this term, the signal is multiplied by $\cos(\sigma t)$. So from Figure 2.7,

$$x(t) = m(t)\cos(\sigma t) \tag{3.65}$$

With some trigonometric manipulation, $x(t)$ can be written as

$$x(t) = \frac{\varepsilon}{2}M'_{\omega_0}[\xi(t)] + q(t), \tag{3.66}$$

where the term $q(t)$ includes higher frequency components around σ, 2σ, $2\omega_0 - \sigma$, $2\omega_0 + \sigma$, $(n-1)w_0 + \sigma$, $(n-1)w_0 + \sigma$, $(n+1)w_0 + \sigma$, and $(n+1)w_0 - \sigma$. Passing the signal $x(t)$ through the low pass filter $F(s)$ attenuates these signals. Assuming these signals are entirely eliminated, it follows that

$$z(t) = \frac{\varepsilon}{2}f(t) * M'_{\omega_0}[\xi(t)], \tag{3.67}$$

where $f(t)$ is the impulse response of the filter $F(s)$ and $*$ is the convolution operation. It follows from 3.51 and 3.67 that

$$\xi_c(t) = \frac{k_\xi \varepsilon}{2} f(t) * M'_{\omega_0}[\xi(t)]. \tag{3.68}$$

Considering that $\xi_c(t) = \xi(t) - \omega_0$, the equation becomes

$$\xi(t) - \xi_0 = \frac{k_\xi \varepsilon}{2} f(t) * M'_{\omega_0}[\xi(t)], \tag{3.69}$$

where

$$\xi(t) = \xi_s(t) - \varepsilon \cos(\sigma t). \tag{3.70}$$

This equation is an approximation of the dynamic behavior of the adjustable parameter in the resonance seeking control system. Therefore, if the system is stable and $F(s)$ contains at least one integrator, $M'_{\omega_0}[\xi(t)]$ will approach a steady state value of zero. Thus the parameter value $\xi(t)$ asymptotically approaches the parameter value ξ_r, or similarly the tuning signal $\xi_s(t)$ asymptotically approaches $\xi_r + \varepsilon \cos(\sigma t)$. Thus, to ensure that the average value of $\xi_s(t)$ at steady state is very close to the parameter value corresponding to resonance ξ_r, ε should be chosen to be sufficiently small.

As in resonance seeking control, the nonlinear equation (3.69) is linearized about the nominal adjustable parameter ξ_0 and about nominal fixed system parameter κ_0 below. $M_{\omega_0}(\xi)$ is denoted $M_{\omega_0}(\xi, \kappa)$ since it is also dependent on κ. Thus linearization yields

$$\delta\xi(t) = kf(t) * [\delta\xi_r - \delta\xi(t)]. \tag{3.71}$$

where

$$k = -\frac{k_\xi \varepsilon}{2} \frac{\partial^2}{\partial \xi^2} M_{\omega_0}(\xi, \kappa)\Big|_{\substack{\xi=\xi_0 \\ \kappa=\kappa_0}} \tag{3.72}$$

and

$$\delta\xi_r = -\frac{\frac{\partial^2}{\partial \kappa \partial \xi} M_{\omega_0}(\xi, \kappa)\Big|_{\substack{\xi=\xi_0 \\ \kappa=\kappa_0}}}{\frac{\partial^2}{\partial \xi^2} M_{\omega_0}(\xi, \kappa)\Big|_{\substack{\xi=\xi_0 \\ \kappa=\kappa_0}}} \delta\kappa. \tag{3.73}$$

Also, $\delta\xi(t) = \xi(t) - \xi_0$ and $\delta\kappa = \kappa - \kappa_0$. Further, $\delta\xi_r$ is the deviation of the tuned parameter from the nominal value ξ_0. Lastly, from equation 3.70 it can be seen that

$$\delta\xi_s(t) = \delta\xi(t) + \varepsilon\cos(\sigma t). \tag{3.74}$$

To further demonstrate these equations, a block diagram is presented in Figure 3.2 that represents the linearized model in equation 3.71. Thus, the closed loop resonance tuning control system behavior can be analyzed with standard linear system techniques, and similar results and methods from resonance seeking control are applicable.

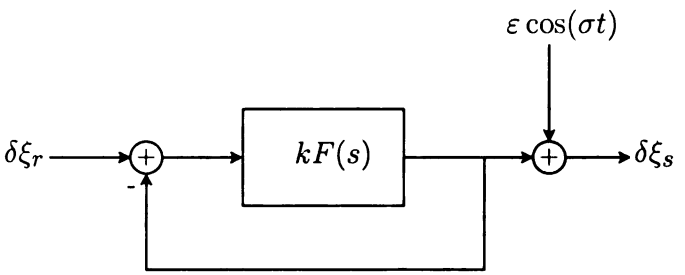

Figure 3.2. Simplified linear model of resonance tuning control system.

CHAPTER 4

Design

In this chapter, the design problem formulated above is considered and some guidelines for designing the resonant frequency control system are provided. Using these guidelines the actual resonant frequency control systems are simulated with the previously discussed parameters of the application. These simulation results illustrate the performance of the resonant frequency control systems and verify the accuracy of the proposed models. All simulations are carried out in MATLAB/Simulink. In addition, experimental results for the RF plasma ignition system are presented to demonstrate its feasibility.

4.1 Design Guidelines

4.1.1 Self-Oscillating Resonance Tracking Design

For second order systems with time delays, as shown in Figure 2.5 the compensator parameter η can be selected using equation (3.14). For a desired output amplitude Y, the design parameter β can be selected using the nominal values of the resonant system as

$$\beta = +\frac{\pi\zeta_n\omega_{n0}Y}{2\gamma_n K} \tag{4.1}$$

when $\omega_{n0}\tau \in (-\pi/2, +\pi/2)$, mod (2π) and

$$\beta = -\frac{\pi\zeta_n\omega_{n0}Y}{2\gamma_n K} \tag{4.2}$$

when $\omega_{n0}\tau \in (+\pi/2, +3\pi/2)$, mod (2π), where ω_{n0}, ζ_n and γ_n are the nominal values of ω_0, ζ and γ, respectively.

In order to self-start the oscillation, the system shown in Figure ?? with $\varphi(u)$ replaced by $N(\alpha)$ must be unstable for sufficiently large $N(\alpha)$. When the amplitude of the output is small, the signum nonlinearity provides the necessary high gain for the fundamental component to self-start the oscillation. The system then generates a periodic waveform with a growing envelope until the signum nonlinearity limits the amplitude of the oscillation to the value estimated by equation (3.8). The transfer function $G(s)$ filters out all but the fundamental component of this periodic waveform yielding an essentially sinusoidal output at the angular frequency estimated by equation (2.5).

It should be pointed out that a higher order compensator $C(s)$ can be used to better compensate for the delay in the loop. Simulation results do, however, indicate that the selected simple compensator is adequate for the intended ignition application. In addition, a static saturation type nonlinearity can also be used in place of the signum nonlinearity for amplitude limiting.

If the system is higher than second order, and a unique solution to the harmonic balance equations exists with simple phase compensator of the form given in equation (2.17), the simple phase lead compensator solution presented above may still be suitable. However, if the disturbances to the resonant system cause large deviations in the natural frequency of the system, requiring more robustness, or the harmonic balance equations yield multiple solutions, a higher order compensator may be required. Notice that the second-order system of equation (2.16) with no time delay and no compensation is robust to disturbance in the natural frequency, as $\angle G(j\omega_n) = 0$ for any ω_n. Thus, using cancelation to convert a system to this form ideally will result in such robustness. Assuming that the dominant poles in the form of equation (2.16)

can be factored out such that

$$\begin{aligned} G(s) &= G_r(s)G_{nr}(s) \\ &= G_{nr}(s)\frac{\gamma s}{s^2 + 2\zeta\omega_n s + \omega_n^2}, \end{aligned} \tag{4.3}$$

it is easily seen that choosing $C(s)$ to directly cancel $G_{nr}(s)$ will yield the robust form discussed above. This is a simple method, but it should be noted that it is often impractical since it may yield improper, unstable, or complicated compensators, or cancelation of unstable zeros or poles. In addition, G_{nr} may have terms that could be considered dominant near the resonant frequency. Thus, careful analysis of the system should be carried out before designing such a compensator. If such a compensator is not suitable, yet more robustness to disturbance to the natural frequency is still needed, using compensator which satisfies the necessary phase condition similar to that in equation (3.11) and one or more of its derivatives may be a viable alternative.

4.1.2 Resonance Seeking Control System

The primary component of the system requiring careful design for the resonance seeking control topology is the low-pass filter. This filter plays a critical role in the control strategy. From the linearized model, it is clear that the filter acts as the controller. Thus, the goal of the resonance seeking control system is to find the 'controller' $F(s)$ such that the 'output' $\omega_s(t)$ tracks the 'input' ω_r satisfactorily. Having obtained this linear model, the use of standard linear control design methods can be used, with the assumption that the linear model is accurate.

The following guidelines should thus be followed when designing such a control system:

- The parameter ε should be sufficiently small so that the it is reasonable to assume the higher-order terms of the Taylor series can be ignored and the perturbation signal applied to $\omega_s(t)$ is negligible.

- The filter $F(s)$ should stabilize the closed loop system shown in Figure 2.6.

- The filter $F(s)$ must contain at least one integrator to achieve near-zero steady-state tracking error.

- The bandwidth of the filter $F(s)$ must be sufficiently small to reject the high frequency terms at σ and ω_0.

- The bandwidth of the filter $F(s)$ should be sufficiently large to reduce settling time of the system.

It should also be noted that the resonance seeking control system can be designed to stabilize about a local minimum in the magnitude response of the resonant system using similar guidelines.

4.1.3 Resonance Tuning Control System

The feedback loop in the resonance tuning control system is very similar to that of the resonance seeking problem, as found in the analytical section. Thus, some of the filter design guidelines will not be restated. As above, the primary component of the system requiring careful design for the resonance tuning control topology is the low-pass filter, and similar guidelines should be followed when designing it. As found previously, from the linearized model, it is clear that the filter acts as the controller. Thus, the goal of the resonance tuning control system is to find the 'controller' $F(s)$ such that the 'output' $\xi_s(t)$ tracks the 'input' ξ_r satisfactorily. This approach allows the use of standard linear control design methods, with the assumption that the linear model is accurate. Like the resonance seeking control method, resonance tuning control systems can be designed to stabilize about a local minimum as well as a local maximum of the magnitude response of the resonant system. The dynamic vibration absorber example is a case when stabilizing about a local minimum is necessary. Simulations for this example are presented below.

4.2 Simulation

4.2.1 Self-Oscillating Resonance Simulation

Simulation results are presented below to compare the ability of the open-loop and closed-loop systems to initiate and sustain robust oscillation at the resonant frequency of the RLC circuit in the RF plasma ignition system. Feasibility of the ignition system will also be assessed by observing trends in timing and magnitude.

The model used for simulation is defined by equations (2.15)-(2.18). Using the guidelines developed earlier, β is selected as $\beta = 5$ and $C(s)$ is designed as

$$C(s) = 1 + 4.73 \times 10^{-9} s. \tag{4.4}$$

With these values, the system shown in Figure 2.5 is simulated by assuming that L and C undergo 5% increase at $t = 50 \times 10^{-6}$ s. The instantaneous amplitude and angular frequency of the capacitor voltage for the closed-loop system are shown in Figure 4.1. For comparison purposes, the same system is also simulated by breaking the loop at the output of the nonlinearity and letting $v(t) = 5\,\mathrm{sgn}\,[\cos(w_0 t)]$ (the nominal driving input). The instantaneous amplitude and angular frequency of the capacitor voltage for the open-loop system are also shown in Figure 4.1. The nominal angular resonant frequency is also plotted in this figure with dashed line for reference. In both cases, the instantaneous amplitude and angular frequency of the capacitor voltage are obtained from the output $y(t)$ numerically.

It should be pointed out that results obtained for closed-loop system from simulation agree well with those calculated based on the previous analysis. Using equation (3.10), the steady-state angular frequency of the output with R, L and C at their respective nominal values is estimated to be 81.63×10^6 rad/s. Using this value in equation (3.8), the steady-state amplitude of the output for this case is estimated to be 21.95 A. The same values are determined from simulation to be 81.62×10^6 rad/s and 21.95 A, respectively. Similarly, with L and C shifted as described above and R

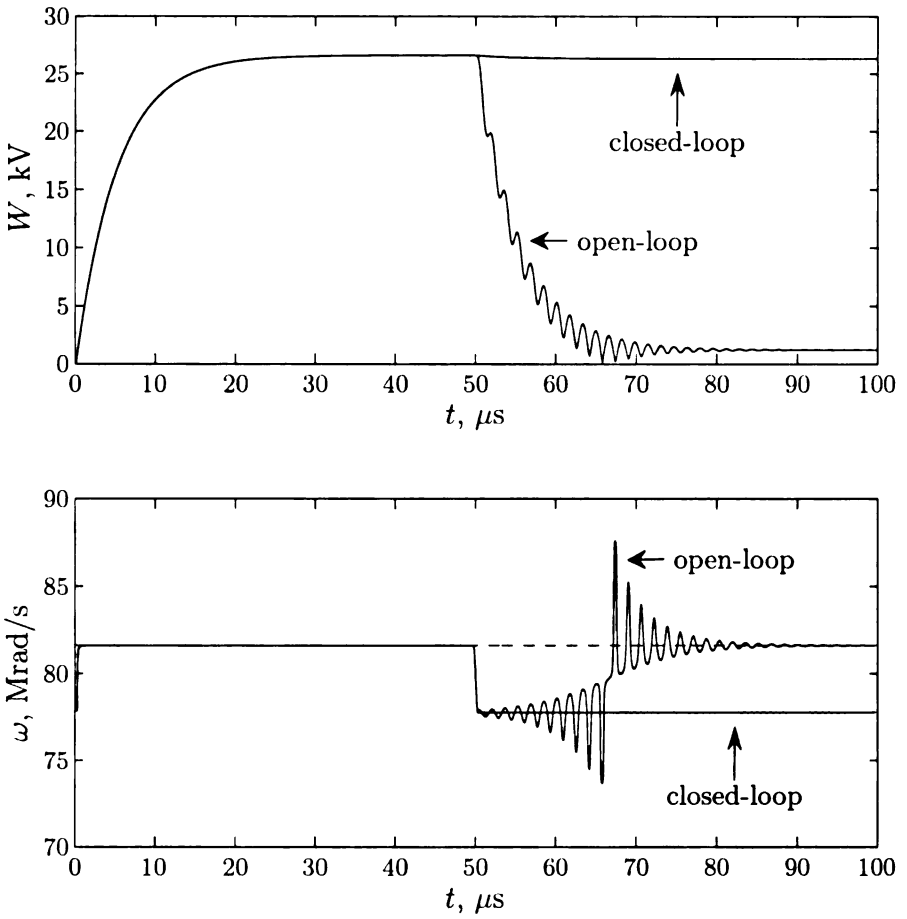

Figure 4.1. Amplitude and angular frequency of the capacitor voltage.

at its nominal value, the steady-state angular frequency and amplitude of the output are estimated to be 77.77×10^6 rad/s and $Y = 21.66$ A, respectively. These values are determined from simulation to be 77.76×10^6 rad/s and 21.71 A, respectively.

These simulation results demonstrate that the analysis and design methods developed above are quite accurate. The performance achieved by the resonance tracking system considered above indicates that the proposed method is a viable solution to the resonance tracking problem.

4.2.2 Resonance Seeking Control Simulation

The RF plasma ignition system is a suitable example for resonance seeking control due to its very distinctive peak in the magnitude response of the RLC circuit corresponding to the natural frequency. Thus, the system model and nominal parameters discussed above will be used for the resonator for simulation of resonance seeking control. The following parameter values were chosen for the system. The loop gain was chosen as $k_\omega = 35 \times 10^{19}$, the system input amplitude as $V = 100$ V, the perturbation frequency as $\sigma = 3.26 \times 10^5$, and the amplitude of the perturbation frequency as $\varepsilon = 81.62 \times 10^3$ rad/s. The filter, $F(s)$ was chosen as

$$F(s) = \frac{1}{s(s^2 + 2.18 \times 10^5 s + 1.18 \times 10^{10})}. \tag{4.5}$$

Figure 4.2 shows the driving frequency ω_s for two different values of initial frequency ω_0, $\omega_0 = 0.98\omega_n$ and $\omega_0 = 1.05\omega_n$, to represent changes in the values of the RLC circuit that result in a shift in the natural frequency. The system effectively tracks natural frequency. Smaller disturbances in the nominal or natural frequencies result in much faster settling. This is due to the high $M'(\omega)$ values that occur locally around the natural frequency, effectively increasing the loop gain, and causing faster settling. That is also the reason for the slow response for the larger deviation. $M'(\omega_s)$ is minimal when ω_s deviates a large amount from ω_0.

Comparing the resonance seeking control system to the self-oscillating resonance tracking control system reveals that the self-oscillating resonance frequency control system is a more suitable control system for implementation due to the simplicity of the control method, as well as the resonance frequency tracking performance. However, resonance seeking control is useful since the algorithm is not limited to second order systems and it is not dependant of the phase of the system, but strictly maximizes the magnitude response of the resonant system.

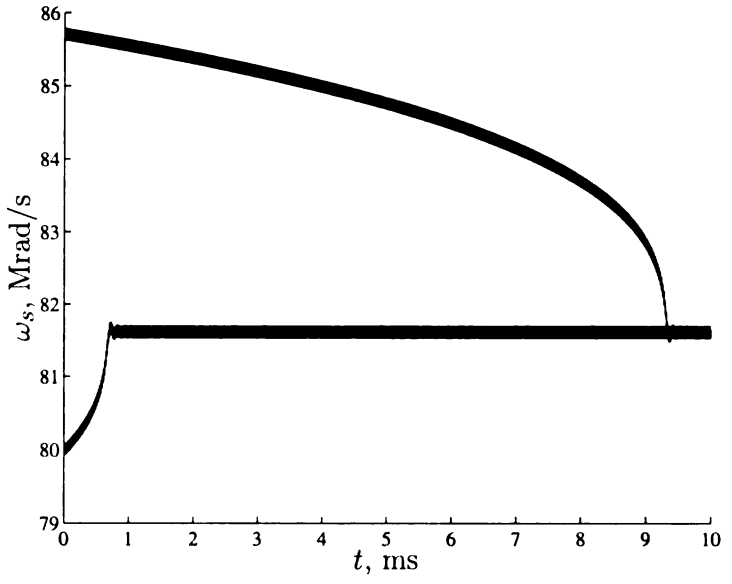

Figure 4.2. Angular frequency response for ignition system.

4.2.3 Resonance Tuning Control Simulation

The classical dynamic vibration absorber problem is ideal for resonance tuning control. Instead of maximizing the magnitude response of the system, however, the vibration absorption problem calls for minimization of the magnitude response of the primary system. For this simulation, the excitation frequency is perturbed from the value to the absorber is tuned, resulting in the following force on the primary mass

$$F = 100 \sin 95t \text{ N}. \tag{4.6}$$

Excitation at this frequency does result in minimal displacement of the primary mass since the absorber is not excited at the frequency for which it was tuned. Thus, a resonance tuning control system with the following parameters is implemented. The loop gain is chosen as $k_\xi = -300$, the perturbation amplitude $\varepsilon = 0.70$ N/m, the perturbation frequency $\sigma = 9.5$ rad/sec, and the nominal parameter value $k_{20} = 200$ N/m. The filter $F(s)$ is chosen to be

$$F(s) = \frac{1}{s(s^2 + 0.9500s + 0.2256)}. \tag{4.7}$$

Figure 4.3 shows the displacement of the primary MSD system $x_p(t)$ based on the above control system. Clearly the system accurately tracks the minimal magnitude response of the system as designed. The steady state amplitude which remains is due to the slight amount of damping in the system. Figure 4.4 shows the input

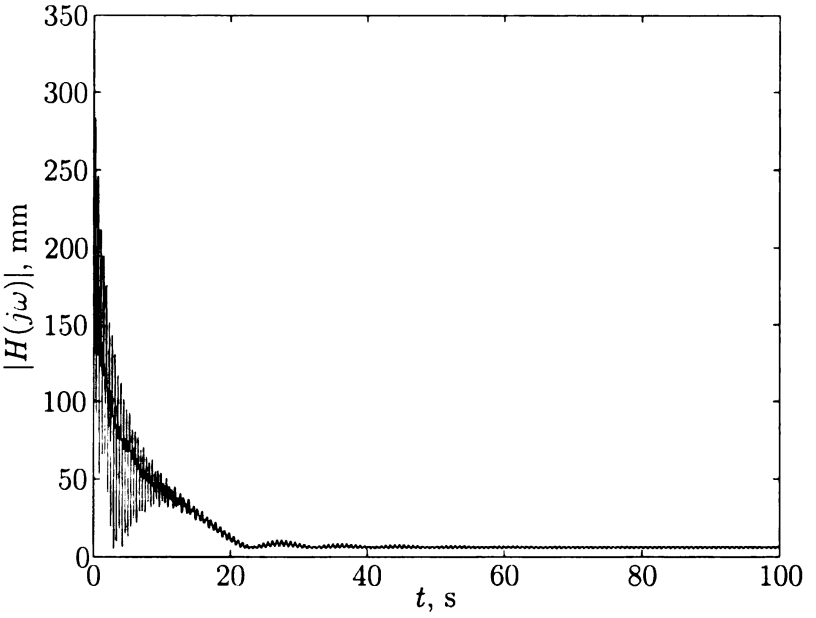

Figure 4.3. Magnitude response of the primary mass.

ξ_s applied to the variable stiffness k_a. The response shows stable tracking of the parameter to minimize the damped mass displacement. Figure 4.5 is a bode plot showing the change in the phase and magnitude characteristics corresponding to the nominal resonant system and the system with the parameter value after the control system reaches steady state. From this plot, it is evident that the control system is effective at tuning the system to the excitation frequency.

Thus, the resonance tuning system is a viable method for tuning the parameters of a resonator to minimize or maximize the magnitude response.

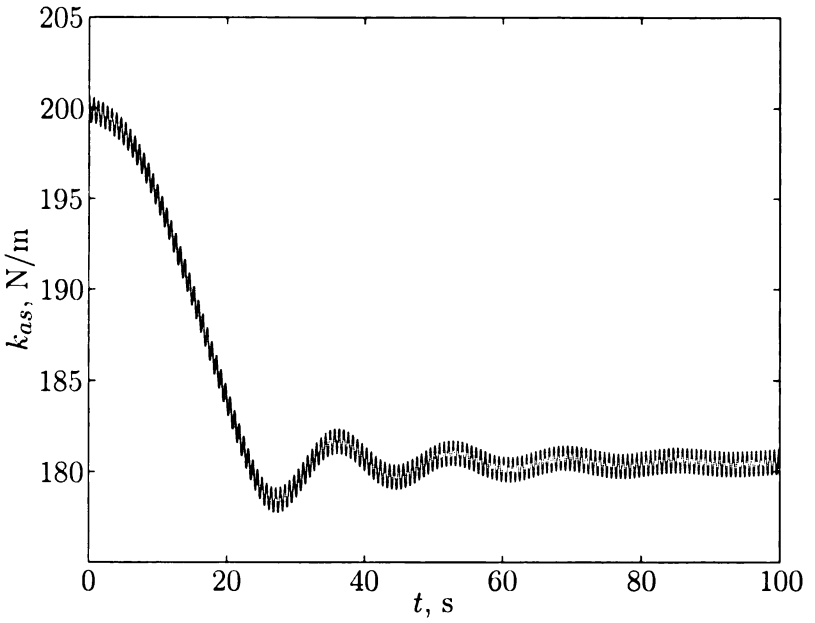

Figure 4.4. Tuned parameter response.

4.3 Experimental Results and Discussion

This section will discuss preliminary experimental results of the primary motivating application, the RF plasma ignition system. To further investigate the feasibility of the ignition system, bench testing and engine testing were performed. Bench testing consisted of developing an open-loop plasma torch generation system capable of accurate timing and duration control. The closed-loop system was also implemented during bench testing after a robust open-loop system had been developed. Engine testing involved taking high-speed video of ignition and combustion events in an optically accessible engine to determine the capabilities and benefits of the system.

The closed loop control topology selected for the ignition system was self-oscillating resonance frequency tracking control due to the simple mature of the control system and the very fast response to parameter perturbations. Figure 4.6 shows the amplitude of the open-loop and closed-loop systems during resonance buildup with low supply voltage to prevent breakdown. As expected, the closed-loop sys-

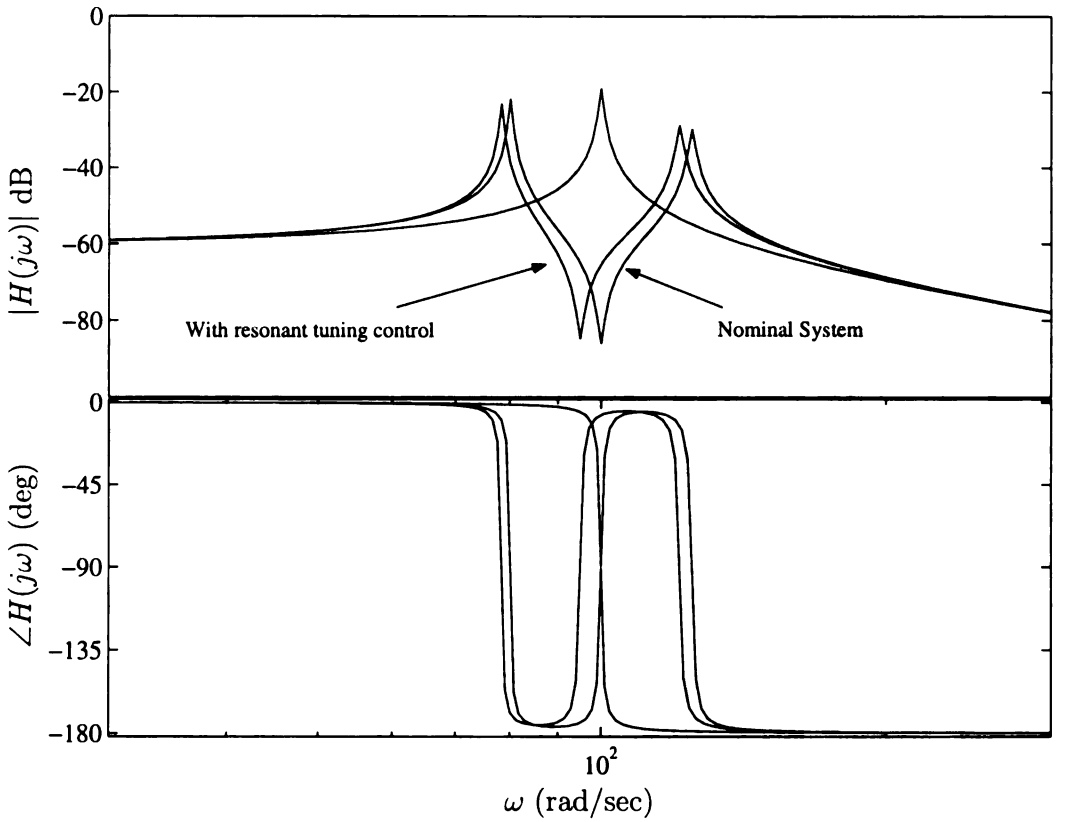

Figure 4.5. Bode plot of MSD with and without dynamic vibration absorber.

tem response has comparable amplitude and response time to the open-loop system response when resonance is manually maintained.

Experimental data also shows that resonance buildup before breakdown occurs in approximately 50 μs depending on the system configuration and breakdown can easily be timed within a 5 μs window. The resonant system clearly has a much faster and more precise response time compared to a conventional inductive ignition system, which has a typical rise time of 300-500 V/μs. This has the potential to reduce cycle-to-cycle variability, to more accurately approach the knock threshold, and to allow more accurate calibration for cylinder-to-cylinder deviations and other issues requiring consistent and accurate ignition events.

The most recent testing of the system has been on a single cylinder, optically ac-

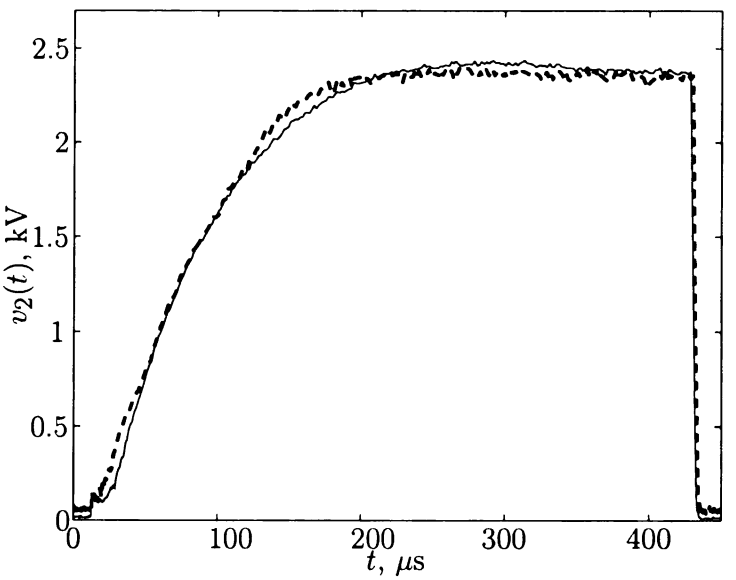

Figure 4.6. Amplitude of voltage across the capacitor V_2 for open-loop (solid) and closed-loop (dashed) systems.

cessible, direct injection, gasoline engine with the ignition system running open-loop. The engine has a quartz window in the piston to allow an axial view of combustion progression. Initial testing was completed in open-loop mode with no fuel being injected to verify that ignition events could occur at high pressures. Following successful completion of these tests, various ranges for ignition timing, ignition duration, and fuel duration were tested. All load, timing and fuel points showed repeated and successful ignition events.

Two images showing the beginning and end of a 4 ms ignition event are shown below. Figure 4.7 shows the commencement of a typical ignition event approximately 150 μs after the start of plasma formation. At this point in the event, the mixture has already begun to burn around the individual plasma streamers. This was determined by analyzing several different combustion videos of similar ignition events. For reference, the estimated diameter of the corona is about 2 cm. Figure 4.8 shows that the flame has already propagated through much of the cylinder before the 4 ms ignition event has even completed.

Figure 4.7. Corona at the beginning of an ignition event.

The ignition system showed excellent ignition characteristics even in very short duration events of less than 150 μs. Lean limits were also tested on the optically accessible engine, and the system consistently ignited the leanest mixtures tested, even in cold start conditions. However, with the equipment available and the very limited number of cycles being run for each test, quantification of limits and potential benefits was not possible.

Figure 4.9 shows the approximate burn time obtained by observing the high speed videos obtained from engine testing. Video was taken of the axial view of the combustion chamber through a quartz window in the piston. The following data is from operation with ignition timing at 12 degrees before top dead center (BTDC) at the engine running at low load. There is clearly a minimum duration of about 0.5 ms to achieve faster burn times with this ignition system, although shorter burn times do effectively and consistently ignite the mixture.

Figure 4.10 shows the approximate burn time obtained by observing the high

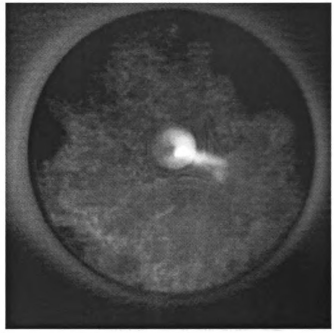

Figure 4.8. Flame propagation at the end of a 4 ms ignition event.

speed videos obtained from engine testing. The affect of ignition timing on the burn duration are as expected, with the 'hook' pattern used for timing optimization present. Comparative data is not currently available for the system, so quantification of the benefits of the RF plasma ignition system is not yet possible.

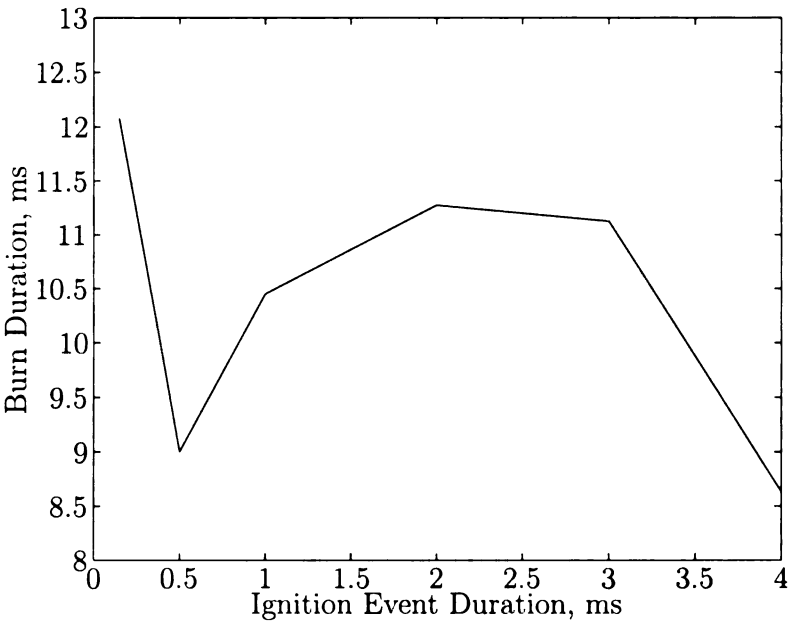

Figure 4.9. Burn time with respect to ignition event duration.

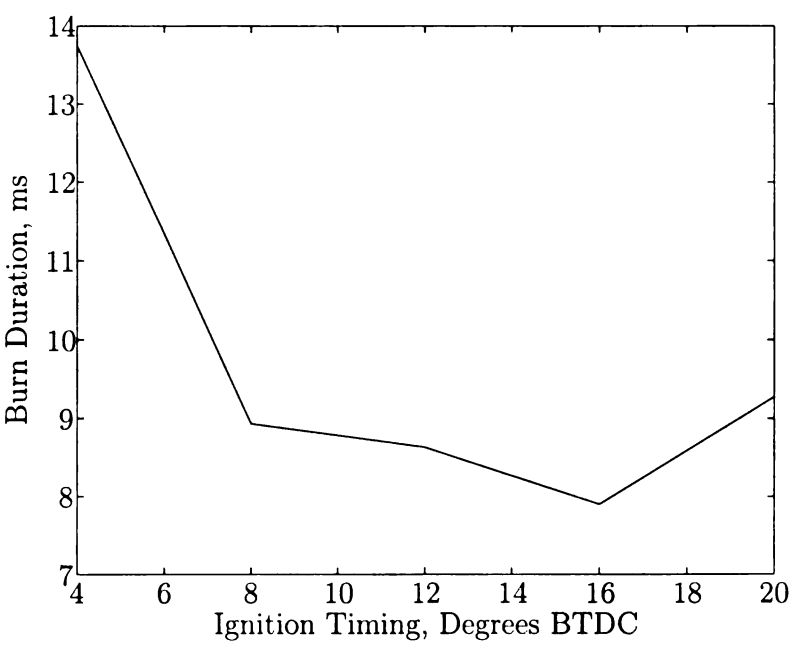

Figure 4.10. Burn time with respect to ignition timing.

CHAPTER 5

Conclusions

5.1 Summary

The primary focus of this thesis is the systematic development of analysis and design methods for three resonant frequency control methods. The first approach to resonant frequency control is through a self-oscillating resonance tracking feedback topology. The second approach utilizes variable frequency excitation to seek the resonant frequency of the system. The last approach varies a parameter in the resonant system to tune the resonant frequency of the resonator to the excitation frequency. Two applications are presented to illustrate the effectiveness of the resonant frequency control systems. The first is a novel resonance-based RF plasma ignition system composed of a high quality factor series RLC circuit driven by an RF generator to start and sustain an RF plasma torch inside the combustion chamber. The second is a dynamic vibration absorber composed of a primary mass-spring-damper system, and tuned absorber consisting of a mass-spring-damper where the spring has variable stiffness.

The self-oscillating resonant frequency control method that is presented utilizes a first-order phase lead compensator to compensate for phase changes in the loop and a nonlinearity is used to achieve amplitude limitation for sustained oscillation. The describing function method is employed for analysis and design of the self-oscillating resonance tracking system, and detailed guidelines are established for the design of

the self-oscillating resonance frequency tracking system for second-order systems with time delays.

The second method of resonant frequency control that is presented is an adaptive method that seeks a local maximum of the magnitude response of the resonant system. This is accomplished by perturbing the driving frequency then synchronously demodulating the absolute value of the output of the resonator to estimate the derivative of the magnitude response with respect to the driving frequency. This derivative is then used for tracking purposes.

The third method of resonant frequency control that is presented is also an adaptive method that seeks a local maximum of the magnitude response of the resonant system, but instead of seeking the maximum frequency, the controller adjusts a parameter of the resonator to cause the resonant frequency of the resonator to track a constant excitation frequency. This is accomplished by perturbing the adjustable parameter and synchronously demodulating the absolute value of the output of the resonator to estimate the derivative of the magnitude response with respect to the driving frequency. The derivative is then used for tracking purposes.

Nonlinear models that accurately predict the performance of the resonant frequency control systems are developed. These developed models are then linearized to obtain more tractable linear time-invariant models that can be used for both analysis and design of the resonant frequency control systems. Based on the developed linear time-invariant models, specific guidelines for designing the resonant frequency control systems are also provided.

Design guidelines are introduced for each resonant frequency control method. Based on these design methods, results from simulation of the RF plasma ignition system and dynamic vibration absorber are presented to illustrate the benefits. Promising results from bench and engine testing of the RF plasma ignition system which indicate that it is feasible for practical applications are also shown. Ignition is very

consistent under pressure and in cold start conditions with relatively small cycle-to-cycle variation. The ignition energy and timing of the developed ignition system can be controlled very precisely. The system generates corona discharges, which are a far more efficient and effective means of ignition than arc discharges. Spark plugs without a ground electrode can therefore be used, reducing the quenching effect the electrodes normally have on the discharge while dispersing the ignition energy over a large volume.

5.2 Future Work

Future theoretical work will include further development of resonant frequency control methods stemming from resonance seeking and resonance tuning control. Methods of combining resonance tracking and resonance tuning control to further enhance resonant frequency control system performance will be researched, as well as improving the adaptive control methods to achieve faster response time. In addition, general methods for systematic analysis and design of self-oscillating resonance tracking control for higher-order systems will be investigated.

Future work also will include investigation of modelling of the ignition system during and after breakdown to provide more effective compensator designs and other types of static nonlinearities for more effective compensation of system parameter changes during operation. This will help optimize the energy transfer to the mixture after breakdown since the breakdown changes the system configuration and natural frequency considerably. Future design work for the RF plasma ignition system will focus on mechanical system development and packaging for on-engine testing so that the benefits of the system can be quantified. Positive results are expected based on the research supporting corona discharge ignition and the testing that has been completed.

BIBLIOGRAPHY

[1] Y. Mizutani, T. Suzuki, H. Ikeda, H. Yoshida, and S. Shinohara,"Frequency control of MOSFET fullbridge power inverter for maximizing output power to megasonic transducer at 3 MHz," *Proc. IEEE Ind. Applicat. Conf.*, St. Louis, MO, pp. 1644-1651, 1998.

[2] S. Furuya, T. Maruhashi, Y. Izuno, and M. Nakaoka, "Load-adaptive frequency tracking control implementation of two-phase resonant inverter for ultrasonic motor," *IEEE Trans. Power Electron.*, 7, pp. 542-550, 1992.

[3] A. Arnau, T. Sogorb, and Y. Jimenez, "A new method for continuous monitoring of series resonance frequency and simple determination of motional impedance parameters for loaded quartz-crystal resonators," *IEEE Trans. Ultrason., Ferroelect., Freq. Contr.*, 48, pp. 617-623, 2001.

[4] J. Phinney and D. J. Perreault, "Filters with active tuning for power applications," *IEEE Trans. Power Electron.*, 18, pp. 636-647, 2003.

[5] Y. S. Kwon, S. B. Yoo, and D. S Hyun, "Half-bridge series resonant inverter for induction heating applications with load-adaptive PFM control strategy," *Proc. IEEE Appl. Power Electron. Conf. and Expo.*, Dallas, TX, pp. 575-581, 1999.

[6] R. P. Leland, "Adaptive mode tuning for vibrational gyroscopes," *IEEE Trans. Contr. Syst. Technol.*, 11, pp. 242-247, 2003.

[7] X. Sun, R. Horowitz, and K.Komvopoulos, "Stability and resolution analysis of a phase-locked loop natural frequency tracking system for MEMS fatigue testing," *ASME J. Dynamic Syst, Meas. Contr.*, 124, pp. 599-605, 2002.

[8] Y. Sun and W. K. Lau, "Antenna impedance matching using genetic algorithms," *Proc. IEE National Conf. Antennas Propagat.*, York, United Kingdom, pp. 31–36, 1999.

[9] Y. Sun and W. K. Lau, "Evolutionary tuning method for automatic impedance matching in communication systems," *Proc. IEEE Int. Conf. Electron., Circuits, Syst.*, Lisboa, Portugal, pp.73–77, 1998.

[10] J. R. Moritz and Y. Sun, "Frequency agile antenna tuning and matching," *Proc. IEE Int. Conf. HF Radio Syst. Tech.,*, Guildford, United Kingdom, pp.169–174, 2000.

[11] S. I. Kwon, A. Regan, and M. Prokop, "Frequency shift observer for an SNS superconducting RF cavity," *IEEE Trans. Nucl. Sci.*, 50, pp. 201-210, 2003.

[12] J. deMingo, A. Valdovinos, A. Crespo, D. Navarro, and P. Garc "An RF electronically controlled impedance tuning network design and its application to anantenna input impedance automatic matching system," *IEEE Trans. Microwave Theory Tech.*, vol.52, no.2, pp. 489–497, 2004.

[13] S. Simrock, G. Petrosyan, A. Facco, V. Zviagintsev, S. Andreoli, and R. Paparella, "First demonstration of microphonic control of a superconducting cavity with a fast piezoelectric tuner," *Proc. IEEE Particle Accel. Conf.*, Hamburg, Germany, pp. 470-472, 2003.

[14] P. Cevc, T. Walczak, and H. M. Swartz, "Whole body L-band resonator with a wide range frequency tuning using piezoactuator," *Current Topics in Biophysics*, 26, pp. 15-19, 2002.

[15] M. Liepe, W. D. Moeller, and S. N. Simrock, "Dynamic Lorentz force compensation with a fast piezoelectric tuner," *Proc. IEEE Particle Accel. Conf.*, Chicago, IL, pp. 1074-1076, 2001.

[16] C. Hovater, J. Delayen, L. Merminga, T. Powers, and C. Reece, "RF control requirements for the CEBAF energy upgrade cavities," *Proc. Int. Linac Conf.*, Monterey, CA, pp. 518-520, 2000.

[17] J. R. Delayen,"Electronic damping of microphonics in superconducting cavities," *Proc. IEEE Particle Accel. Conf.*, Chicago, IL, pp. 1146-1148, 2001.

[18] F. Braun and W. Arnold, "Fast matching of load changes in the ion cyclotron resonance frequency range," *Proc. IEEE Sympo. Fusion Engin.*, Albuquerque, NM, pp. 395-398, 1999.

[19] K. Akai, N. Akasaka, E. Ezura, T. Kageyama, H. Mizuno, F. Naito, H. Nakanishi, Y. Takeuchi, Y. Yamazaki, and T. Kobayashi, "Tuning control and transient response of the ARES for KEKB," *Proc. IEEE Particle Accel. Conf.*, Sitgas, Spain, pp. 1994-1996, 1996.

[20] T. Sumesaglam, A. I. Karsilayan, "A digital approach for automatic tuning of continuous-time high-Q filters," *IEEE Trans. Circuits Syst. II,* 50, pp. 755-761, 2003.

[21] C. Gökçek, "Tracking the resonance frequency of a series RLC circuit using a phase locked loop," *Proc. IEEE Conf. Contr. Appl.,* pp. 609–613, 2003.

[22] J. A. Jeltema and C. Gökçek, "Adaptive resonance tuning through feedback," *Proc. Amer. Contr. Conf.*, Portland, OR, 2005.

[23] J. A. Jeltema, J. Ma, C. Gökçek, "Analysis and design of resonance tuning systems," *Optomechatronic Sensors, Actuators, and Control. Proceedings of the SPIE*, Volume 5602, pp. 122–132, 2004.

[24] G. J. Rohwein, S. R. Babcock, M. T. Buttram, and L. S. Camilli, "Advanced automotive ignition system," *Enerpulse Inc., http://www.directhits.com,* 2006.

[25] A. Y. Starikovskii, "Plasma supported combustion," *Invited Topical Review, Proc. Combustion Institute,* 30, 2005.

[26] S. M. Starikovskaia, A. V. Kosarev, A. V. Krasnochub, E. I. Mintoussov, and A. Y. Starikovskii, "Control of combustion and ignition in hydrocarbon-containing mixtures by nanosecond pulsed discharges," Proc. AIAA Aerospace Sciences Meeting and Exhibit, Reno, NV, 2005.

[27] R. Maly, B. Saggau, E. Wagner, and G. Ziegler, "Prospects of ignition enhancement," *SAE Paper 830478,* 1983.

[28] R. Maly "Spark ignition: its physics and effects on the internal combustion process," *Fuel Economy in Road Vehicles Powered by Spark Ignition Engines,* Eds., J. C. Hilliard and G. S. Springer, NY: Plenum, 1984.

[29] R. W. Anderson and J. R. Asik, "Lean air-fuel ignition system comparison in a fast-burn engine," *SAE Paper 850076,* 1985.

[30] R. W. Anderson, "The effect of ignition system power on fast-burn engine combustion," *SAE Paper 870549,* 1987.

[31] R. C. Pate and R. E. Hensley, "Combustion initiation system employing hard discharge ignition," *United States Patent No: US4589398,* 1986.

[32] R. Matthews, "Railplug ignition system," *University of Texas, www.eere.energy.gov/de/pdfs/univ-recip-engines-conf-03,* 2003.

[33] Woodward, "Smartfire ignition system," *www.woodward.com/engine /smart-fire.cfm,* 2006.

[34] Knite Inc., "Kinetic Spark Ignition System," *www.knite.com,* 2006.

[35] B. Gunther, "High frequency ion current measurement after AC current ignition," *European Patent No: EP0801294,* 1997.

[36] B. Holz, "Method and device for the transmission of thermal energy to a space filled with matter," *European Patent No: EP0211133,* 1987.

[37] University of Tennessee, "Laser induced ignition," *cla.utsi.edu/Research/Fluid_Physics/Laser_Induced_Ignition.htm,* 2006.

[38] J. B. Liu, F. Wang, L. Lee, P. D. Ronney, M. A. Gundersen, "Effect of fuel type on flame ignition by transient plasma discharges," *42nd AIAA Aerospace Sciences Meeting, AIAA Paper No. 2004-0837,* Reno, NV, 2004.

[39] J. B. Liu, F. Wang, L. Lee, P. D. Ronney, M. A. Gundersen, "Effect of discharge energy and cavity geometry on flame ignition by transient plasma," *42nd AIAA Aerospace Sciences Meeting, AIAA Paper No. 2004-1011,* Reno, NV, 2004.

[40] C. Ting-Kong *Design of an Adaptive Dynamic Vibration Absorber* Masters Thesis, University of Adelaide, Southern Australia, 1999.

[41] M. J. Brennan, "Vibration control using a tunable vibration neutralizer." *Proceedings of the Institution of Mechanical Engineers, Journal of Mechanical Engineering Science* 211, pp. 91-108, 1997.

[42] A. H. Von Flotow, A. Beard and D. Bailey, "Adaptive tuned vibration absorbers: tuning laws, tracking agility, sizing and physical implementations." *Proceedings of Noise-Conference* 94, pp. 437-454, 1994.

[43] J. Q. Sun, M. A. Norris and M. R. Jolly, "Passive, adaptive and active tuned vibration absorbers - a survey." *Transactions of the American Society of Mechanical Engineers (Journal of Mechanical Design) 117,* pp. 234-242, 1995.

[44] P. L. Walsh and J. S. Lamancusa, "A variable stiffness vibration absorber for the minimisation of transient vibrations." *Journal of Sound and Vibration* 158, pp. 195–211, 1992.

[45] W. T. Thomson, M. D. Dahleh *Theory of Vibrations with Applications,* Prentice-Hall, Upper Saddle River, NJ, 1998.

[46] H. K. Khalil, *Nonlinear Systems Analysis.* NJ: Prentice-Hall, 1996.

[47] C. Gökçek, " Resonance Seeking Control," *IEEE/ASME International Conference on Advanced Intelligent Mechatronics. Proceedings,* pp. 1348–1353, 2005.

[48] D. Smith, C. Gökçek, "Self-Oscillating Resonance Tracking Ignition System Design Using the Method of Describing Function" *IEEE Proc. American Control Conference,* New York City, New York, 2007.

[49] D. Smith, "Design and Testing of RF Plasma Ignition System with Self-Oscillating Resonance Tracking" *In preparation.*

[50] K. K. Clarke, and D. T. Hess *Communication Circuits Analysis and Design,* Addison-Wesley Publishing Co., Inc. 1971.

[51] B. Crowell *Vibrations and Waves* Light and Matter, Fullerton, CA, 2006.

[52] C. L. Phillips and R. D. Harbor, *Feedback Control Systems*, 4^th ed., Prentice Hall, 2000.